

1970

The crystal structure determinations of tetraethylammonium hexabromoantimonate (V), 4-ethylpyridinium tetrabromoferrate (III), and D-glucono-(1,5)-lactone, and a method for partial structure evaluation

Marvin LeRoy Hackert
Iowa State University

Follow this and additional works at: <https://lib.dr.iastate.edu/rtd>

 Part of the [Physical Chemistry Commons](#)

Recommended Citation

Hackert, Marvin LeRoy, "The crystal structure determinations of tetraethylammonium hexabromoantimonate (V), 4-ethylpyridinium tetrabromoferrate (III), and D-glucono-(1,5)-lactone, and a method for partial structure evaluation " (1970). *Retrospective Theses and Dissertations*. 4310.

<https://lib.dr.iastate.edu/rtd/4310>

This Dissertation is brought to you for free and open access by the Iowa State University Capstones, Theses and Dissertations at Iowa State University Digital Repository. It has been accepted for inclusion in Retrospective Theses and Dissertations by an authorized administrator of Iowa State University Digital Repository. For more information, please contact digirep@iastate.edu.

71-7271

HACKERT, Marvin LeRoy, 1944-

THE CRYSTAL STRUCTURE DETERMINATIONS OF
TETRAETHYLAMMONIUM HEXABROMOANTIMONATE(V),
4-ETHYLPYRIDINIUM TETRABROMOFERRATE(III),
AND D-GLUCONO-(1,5)-LACTONE, AND A METHOD FOR
PARTIAL STRUCTURE EVALUATION.

Iowa State University, Ph.D., 1970
Chemistry, physical

University Microfilms, Inc., Ann Arbor, Michigan

THE CRYSTAL STRUCTURE DETERMINATIONS OF
TETRAETHYLAMMONIUM HEXABROMOANTIMONATE(V), 4-ETHYLPYRIDINIUM
TETRABROMOFERRATE(III), AND D-GLUCONO-(1,5)-LACTONE,
AND
A METHOD FOR PARTIAL STRUCTURE EVALUATION

by

Marvin LeRoy Hackert

A Dissertation Submitted to the
Graduate Faculty in Partial Fulfillment of
The Requirements for the Degree of
DOCTOR OF PHILOSOPHY

Major Subject: Physical Chemistry

Approved:

Signature was redacted for privacy.

In Charge of Major Work

Signature was redacted for privacy.

Head of Major Department

Signature was redacted for privacy.

Dean of Graduate College

Iowa State University
Of Science and Technology
Ames, Iowa

1970

TABLE OF CONTENTS

	Page
INTRODUCTION	1
THE STRUCTURE OF TETRAETHYLAMMONIUM HEXABROMOANTIMONATE(V)	3
Introduction	3
Experimental	4
Solution and Refinement	6
Description and Discussion of the Structure	10
THE STRUCTURE OF 4-ETHYLPYRIDINIUM TETRABROMOFERRATE(III)	15
Introduction	15
Experimental	15
Solution and Refinement	17
Description of the Structure	20
THE CRYSTAL AND MOLECULAR STRUCTURE OF D-GLUCONO-(1,5)-LACTONE	28
Introduction	28
Experimental	28
Solution and Refinement	31
Description of the Structure	37
Discussion	50
A METHOD FOR PARTIAL STRUCTURE EVALUATION	54
Introduction	54
The Discriminator Function	55
Experimental	60
Results	61
Discussion	74
RESEARCH PROPOSALS	79

LITERATURE CITED

81

ACKNOWLEDGMENTS

85

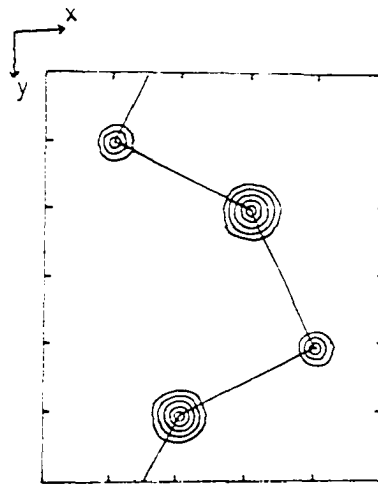
INTRODUCTION

The crystal structures of tetraethylammonium hexabromoantimonate(V), 4-ethylpyridinium tetrabromoferrate(III), and D-glucono-(1,5)-lactone were determined by single crystal X-ray diffraction techniques. The nature and importance of their solid state structures will be discussed. In addition, a new method for partial structure evaluation is presented with experimental results and comments regarding its possible limitations and extensions.

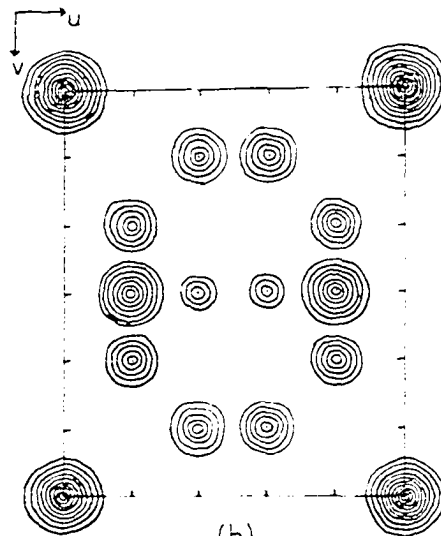
The crystal structure of $(C_2H_5)_4NSbBr_6$ was solved by the conventional heavy-atom technique. The position of the $SbBr_6$ group was found from the Patterson and its orientation was used to select the proper choice of space group. The cation atoms were found to be two-fold disordered from the calculated electron density map. The crystal structure of $C_7H_9NHF_4$ was determined by Patterson superposition techniques. The structure contains a possible weak N-H...Br hydrogen bond. The structure of the lactone was determined using a pseudo-electron density symmetry map in conjunction with the Patterson superposition technique. The restraint of the planar carbonyl group imposes a distorted half-chair conformation on the delta-lactone ring system.

The methods employed in the solution of the above structures illustrate the power and usefulness of the Patterson function¹ in crystallography. Since some familiarity with this function is essential to understanding the above methods as well as the method presented for partial structure evaluation, a simple, hypothetical example is given in Figure 1 and will be used throughout to illustrate the various techniques discussed.

Polymeric CO

Monoclinic $P2_1$, $Z=2$
 $(x, y, z ; \bar{x}, \frac{1}{2}y, \bar{z})$ C $(1/5, 1/6, z)$ O $(3/5, 2/6, z)$ 

(a)



(b)

Figure 1. The (a) electron density and (b) Patterson maps for the hypothetical polymeric carbon monoxide example. The Patterson function is an autocorrelation function of electron density with maxima corresponding to all interatomic vectors

THE STRUCTURE OF TETRAETHYLAMMONIUM HEXABROMOANTIMONATE(V)

Introduction

The crystal structure investigation of tetraethylammonium hexabromoantimonate(V) was undertaken as part of a series of investigations of halo-coordinated antimony compounds being performed in this Laboratory.²⁻⁹ The synthesis of intensely colored compounds of the type $R_xSb_yBr_z$, where R represents either an aliphatic or aromatic amine, has been known since 1901 when Rosenheim and Stellman¹⁰ reported the preparation of $(C_5H_5NH)_2SbBr_7$. Since then a wide variety of such compounds has been reported:¹¹ $RSbBr_4$; $RSbBr_6$; $RSbBr_7$; R_2SbBr_5 ; R_2SbBr_6 ; R_2SbBr_7 ; R_2SbBr_8 ; R_2SbBr_9 ; R_3SbBr_6 ; $R_3Sb_2Br_9$; $R_3Sb_2Br_{11}$; $R_3Sb_2Br_{12}$; $R_3Sb_2Br_{15}$; $R_5Sb_3Br_{14}$; $R_7Sb_3Br_{16}$; and $R'SbBr_3 \cdot 3HBr$. It is believed that the dark color may be due to the presence of mixed oxidation states of antimony or to some other type of charge transfer phenomena. A series of intervalence antimony bromide complexes of varying stoichiometries has been investigated to relate, if possible, their crystal structures and charge transfer properties, and to evaluate the effects of cation size, type and stereochemistry on the antimony bromide anion and on the resulting solid state structure.

The structure of tetraethylammonium salt was undertaken as a result of preliminary investigations on the physical and chemical properties of this material and other intensely colored $R_xSb_yBr_z$ complexes. The tetraethylammonium complex was shown to be unusually stable in comparison to the other antimony-bromide complexes studied, being stable in air and

more slowly hydrolyzed in water. Although the tetraethylammonium complex is also intensely colored,¹² appearing a deep, dark red-brown, the preliminary X-ray results indicated the stoichiometry was $\text{RSb}^{\text{V}}\text{Br}_6$ with only four formula units per unit cell. The usual intervalence type charge transfer could not occur if indeed all the SbBr_6 species present were equivalent. Also, the saturated cation would not be expected to participate in any possible charge transfer path.

Experimental

Crystal data:

Tetraethylammonium hexabromoantimonate(V), $(\text{C}_2\text{H}_5)_4\text{NSbBr}_6$,

$M = 479.5$, Tetragonal $I4_1md$, $F(000) = 1344e$, $Z = 4$,

$a = b = 8.7008(7)$, $c = 24.797(2)\text{\AA}$, $T \approx 24^\circ\text{C}$, $V = 1877.3\text{\AA}^3$,

$D_m = 2.62 \text{ g/cc}$, $D_c = 2.59 \text{ g/cc}$, Mo $K\alpha(\lambda = 0.7107\text{\AA})$, $\mu = 150.7\text{cm}^{-1}$

The $(\text{C}_2\text{H}_5)_4\text{NSbBr}_6$ salt was prepared by the method of Lawton.⁴

Microscopic examination revealed the four-fold symmetry of the crystals, square pyramidal with sharply defined faces. Although the tetraethylammonium salt was observed to be air stable, crystals were selected and mounted in thin-walled Lindemann glass capillaries to limit exposure to the atmosphere. Preliminary Weissenberg and precession photographs exhibited $\frac{4}{m}$ Laue symmetry, indicating a tetragonal space group. The following systematic absences were observed: hkl when $h + k + l = 2n + 1$ and hhl when $2h + l = 4n + 1$. The absences are consistent with either space group $I4_1md$ or $I\bar{4}2d$. The unit cell parameters and their standard deviations were obtained by a least squares fit¹³ to twelve independent

reflection angles whose centers were determined by a left-right, top-bottom beam splitting technique using a previously aligned Hilger-Watts four circle diffractometer (Mo K α radiation, $\lambda = 0.71069\text{\AA}$). The observed density was determined by flotation techniques using ethylene bromide and 1,1,2,2-tetrabromoethane solutions.

A crystal having approximate dimensions $0.10 \times 0.10 \times 0.09\text{mm}$ was mounted on a glass fiber such that the c axis (0.09mm) was nearly coincident with the spindle axis. Data were collected at room temperature utilizing a Hilger-Watts four circle diffractometer equipped with scintillation counter and using Zr-filtered Mo K α radiation. Within a two theta sphere of 60° all data in one full octant were recorded using a θ - 2θ step scan technique with a take-off angle of 4.5° . Symmetric scan ranges of 1.00° in 2θ at low two-theta values to 2.20° at the high two theta limit were used. Stationary crystal - stationary counter background measurements were made at the beginning and end of the step scan, each measurement being made for one-half the total scan time. The counting rate used was 0.2048 sec per step of 0.02° in two theta. The rest of the experimental arrangement used has already been discussed in some detail.¹⁴ A total of 1535 reflections were measured in this way. Three standard reflections were observed periodically and these observations indicated that no decomposition occurred during the data collection.

The intensity data were also corrected for Lorentz-polarization effects and for effects due to absorption ($\mu = 150.7 \text{ cm}^{-1}$). The absorption correction¹⁵ was made using ABCOR;¹⁶ the maximum and minimum transmission factors were 0.414 and 0.322, respectively. The estimated error in each intensity was calculated by

$$\overline{[G(I)]^2} = \overline{[C_T + C_B + (0.03C_T)^2 + (0.05C_B)^2 + (0.04C_R)^2]} / A^2$$

where C_T , C_B , C_R and A are the total count, background count, net count and transmission factor, respectively. The equivalent values of F_o^2 were then averaged. The estimated standard deviation in each structure factor was calculated from the mean deviation in intensity by the method of finite differences.¹⁷ The reciprocals of the structure factor variances were used as weights in the least-squares refinement. Based on the measurements of symmetry extinct data, it was decided that only those reflections with $I > 2\sigma(I)$ would be considered observed. The results reported are based on the remaining 276 independent reflections.

Solution and Refinement

The structure was solved by conventional heavy atom techniques.¹⁸ With only four formula units per unit cell, the antimony and nitrogen atoms must lie in special positions having either mm ($I4_1md$) or $\bar{4}$ ($I\bar{4}md$) site symmetry. The orientation of the hexabromoantimonate(V) group was obtained from a three-dimensional Patterson map and indicated that the space group was $I4_1md$. These heavy atom positions were then refined isotropically by full matrix least-squares techniques using a modified version of OR FLS¹⁹ to a conventional discrepancy factor of $R = \sum(|F_o| - |F_c|) / \sum |F_o| = 0.081$ and a weighted R-factor of $R_w = (\sum_w (|F_o| - |F_c|)^2 / \sum_w |F_o|^2)^{1/2} = 0.194$. The remaining nonhydrogen atoms were found by an electron density map calculation.²⁰

A tetraethylammonium group has two preferred orientations, the swastika configuration or a trans arrangement. Although found in a

trans arrangement, the inner carbon atoms do not lie on the mirror planes and are two-fold disordered. These inner carbons were refined with half occupancy in a general sixteen-fold position. The outer carbons appeared to lie on the mirror planes and were treated as ordered and restrained to these mirror planes. Subsequent refinement using anisotropic thermal parameters for only the heavy atoms lowered the R-factor to 0.042 and $R_w = 0.044$.

The relativistic Hartree-Fock X-ray scattering factors for neutral atoms of Doyle and Turner²¹ were used with those of antimony and bromine modified for the real and imaginary parts of anomalous dispersion.²² Based on the agreement of the large structure factors, no extinction correction was necessary. A final electron density difference map showed no peak heights greater than $0.3e^-/\text{Å}^3$. The final standard deviation for an observation of unit weight $(\sum \omega \Delta^2 / (NO - NV))^{1/2}$ where $\Delta = |F_o| - |F_c|$, NO is the number of observations (276) and NV is the number of variables (38) was 0.95 electrons. During the final cycle the largest shift in any parameter was less than 0.01 times its own e.s.d. The final positional and thermal parameters are given in Table 1, along with their standard deviations as derived from the inverse matrix of the final least-squares cycle. In Figure 2 are listed the magnitudes of the observed and calculated structure factors in electrons x 10. The computer drawings shown throughout the text were made using ORTEP.²³ Distances and angles with standard deviations were calculated using the variance-covariance matrix from the final least-squares cycle and ORFFE program.²⁴

Table 1. Final atomic positional^a and thermal parameters^b and their standard errors^c for (C₂H₅)₄NSbBr₆

Atom	Position	x	y	z	B or β_{11}	β_{22}	β_{33}	β_{12}	β_{13}	β_{23}
Sb	4a	0 ^{*d}	0 [*]	0 [*]	87(5)	117(6)	13(1)	0 [*]	0 ^{**}	0 [*]
Br(1)	8b	0 [*]	0.2034(7)	0.0732(2)	244(12)	217(11)	22(1)	0 [*]	0 [*]	-29(3)
Br(2)	8b	0 [*]	-0.2057(6)	-0.0734(2)	135(8)	155(8)	20(1)	0 [*]	0 [*]	-16(2)
Br(3)	8b	0.2940(4)	0 [*]	-0.0027(3)	97(6)	175(7)	24(1)	0 [*]	-13(3)	0 [*]
N	4a	0 [*]	0 [*]	0.4333(16)	4.0(9)					
C(1)	8b	0.2158(52)	0 [*]	0.3666(17)	5.9(10)					
C(2)	8b	0.2170(47)	0 [*]	0.5064(23)	5.5(10)					
C(3) ^e	16c	0.1005(64)	0.1185(62)	0.3976(18)	4.1(11)					
C(4)	16c	0.0999(63)	-0.0998(70)	0.4684(21)	5.0(11)					

^aPositional parameters are in fractional unit cell coordinates.

^b β 's $\times 10^4$; The form of the anisotropic temperature factor is

$$\exp[-(\beta_{11}h^2 + \beta_{22}k^2 + \beta_{33}l^2 + 2\beta_{12}hk + 2\beta_{13}hl + 2\beta_{23}kl)].$$

^cEstimated standard deviations are given in parentheses for the least significant figures.

^dAsterisk (*) denotes an atomic parameter fixed by symmetry.

^eAtoms C(3) and C(4) are disordered and were refined with half occupancy.

L = 0	0 0 3127 3028	2 0 1234 1223	7 5 748 711	7 1 560 576
H K FO FC	2 0 1724 1675	4 0 509 505	6 6 671 581	3 3 1634 1588
2 0 2729 2709	4 0 2033 1975	3 1 555 586		7 3 756 757
4 0 4762 4826	6 0 1043 1035	2 2 1751 1853	L = 13	
6 0 2388 2476	8 0 510 565	4 2 1050 1074	H K FO FC	L = 19
8 0 898 884	10 0 605 594	6 2 925 364	1 0 2444 2575	H K FO FC
10 0 1134 1217	3 1 444 395	4 4 955 640	3 0 2243 2256	1 0 698 703
3 1 2867 2823	7 1 505 455	6 4 520 537	5 0 1535 1571	3 0 1115 1197
5 1 1291 1281	2 2 620 591	6 6 507 450	7 0 1047 1074	2 1 845 815
7 1 1286 1305	4 2 1116 1107	8 8 584 199	2 1 972 883	3 2 1129 1141
2 2 4015 3905	6 2 564 535		4 1 1004 980	7 2 614 581
5 3 2453 2488	5 3 554 542	L = 9	6 1 650 644	4 3 801 833
9 3 568 555	4 4 1361 1335	H K FO FC	3 2 864 849	7 4 526 448
4 4 2649 2728	6 4 779 768	1 0 1372 1409	5 2 974 988	L = 20
6 4 1366 1395		3 0 1942 1759	4 2 972 1005	H K FO FC
10 4 564 699	L = 5	5 0 814 781	6 3 705 663	2 0 539 582
7 5 1157 1217	H K FO FC	7 0 1063 1084	5 4 1050 1013	3 1 450 418
6 6 809 711	1 0 1824 1905	2 1 1338 1331	7 4 540 592	2 2 1075 1104
	3 0 2480 2437	4 1 711 758	6 5 597 612	4 2 627 646
	5 0 819 753	6 1 534 564		
	7 0 963 990	3 2 1933 1877	L = 14	
L = 1	2 1 1391 1410	5 2 472 486	H K FO FC	L = 21
H K FO FC	4 1 643 648	7 2 978 1060	2 0 926 929	H K FO FC
1 0 2949 3216	6 1 390 396	4 3 1170 1115	1 1 1364 1400	1 0 452 483
3 0 3468 3370	3 2 2285 2227	6 3 984 960	3 1 797 809	3 0 783 811
5 0 2291 2310	5 2 736 682	8 3 547 454	5 1 1308 1330	2 1 702 670
7 0 1425 1449	7 2 1090 1120	5 4 562 474	4 2 471 408	3 2 829 863
9 0 542 524	4 3 1569 1582	7 6 618 607	5 3 700 679	5 2 453 343
2 1 1500 1438	6 3 935 957		5 5 854 838	4 3 605 582
4 1 1719 1655	7 4 610 725	L = 10	7 5 524 391	
6 1 877 916		H K FO FC		L = 22
3 2 1143 1140	L = 6	2 0 1861 1894	L = 15	H K FO FC
5 2 1440 1492	H K FO FC	6 0 597 581	H K FO FC	2 0 1200 1249
7 2 490 540	2 0 5622 5652	1 1 918 991	1 0 1595 1675	3 1 722 727
4 3 1402 1390	4 0 1118 1148	3 1 1451 1402	3 0 1460 1422	4 2 753 746
6 3 664 719	6 0 985 1010	7 1 1031 987	5 0 1002 1019	3 3 977 1017
5 4 1207 1253	8 0 1130 1111	4 2 1146 1148	7 0 694 799	7 3 581 640
7 4 778 775	1 1 324 282	3 3 1755 1787	2 1 472 445	L = 23
6 5 773 778	3 1 2392 2403	5 3 351 558	4 1 886 857	H K FO FC
	5 1 1075 1030	7 3 1048 1076	5 2 615 643	1 0 462 440
L = 2	7 1 1220 1269	7 5 519 468	4 3 944 950	3 0 526 513
H K FO FC	4 2 2470 2429	7 7 651 625	5 4 763 750	3 2 601 628
1 1 2555 2549	6 2 1153 1171	L = 11	6 5 569 439	
3 1 1407 1434	10 2 704 654	H K FO FC		L = 24
5 1 1107 1077	3 3 3771 3868	1 0 1781 1781	L = 16	H K FO FC
7 1 792 811	5 3 427 440	3 0 1496 1505	H K FO FC	0 0 889 886
3 3 1147 1149	7 3 1793 1840	5 0 1117 1065	0 0 2033 2093	2 0 471 522
5 3 968 981	8 4 541 541	7 0 789 769	2 0 989 982	4 0 588 543
7 3 744 694	5 5 1276 1178	4 1 1043 993	4 0 2113 2160	6 0 683 538
5 5 837 910	7 5 545 445	6 1 588 616	6 0 914 973	4 4 541 258
7 5 590 564	7 7 866 937	3 2 639 654	3 1 576 627	6 6 603 296
		5 2 528 459	5 1 468 425	
	L = 7	7 2 454 449	7 1 529 546	
	H K FO FC	4 3 769 755	2 2 827 768	L = 25
L = 3	1 0 2043 2053	6 3 607 560	4 2 638 631	H K FO FC
H K FO FC	3 0 2690 2656	5 4 625 578	5 3 762 753	1 0 755 696
3 0 2480 2447	5 0 1383 1326		4 4 1271 1283	3 0 621 547
5 0 1534 1517	7 0 1163 1164	L = 12	6 4 592 561	
7 0 1239 1327	2 1 2257 2182	H K FO FC		L = 26
9 0 509 539	4 1 492 498	0 0 4725 4890	L = 17	H K FO FC
4 1 1396 1316	3 2 3119 2996	2 0 1452 1455	H K FO FC	1 1 610 562
6 1 558 552	5 2 1168 1076	4 0 2605 2693	1 0 951 925	5 1 543 442
3 2 1110 1142	7 2 1381 1395	6 0 1681 1707	3 0 907 955	L = 28
5 2 411 435	4 3 1728 1657	10 0 748 743	5 0 489 532	H K FO FC
7 2 841 818	6 3 1102 1106	3 1 1600 1607	7 0 544 467	0 0 1213 1108
4 3 1525 1533	8 3 762 742	5 1 732 738	4 1 525 605	2 0 478 386
6 3 785 807	5 4 526 441	7 1 704 781	3 2 438 466	4 0 689 669
8 3 507 478	7 4 863 865	2 2 1354 1359	4 3 671 708	4 4 590 482
5 4 644 659	7 6 656 603	5 3 1452 1498	L = 18	
7 4 902 859		4 4 1328 1312	H K FO FC	L = 30
	L = 8	6 4 916 862	2 0 1189 1231	H K FO FC
L = 4	H K FO FC	10 4 634 492	3 1 1062 1088	3 3 561 308
H K FO FC	0 0 634 636			

Figure 2. Observed and calculated structure factors ($\times 10$) for $(C_2H_5)_4NSbBr_6$

Description and Discussion of the Structure

The crystal structure of tetraethylammonium hexabromoantimonate(V) is shown in Figure 3. Bond distances and angles of interest are given in Table 2 and Figure 4. The $\text{Sb}^{\text{V}}\text{Br}_6^-$ ion has crystallographic C_{2v} symmetry, but is somewhat distorted from O_h symmetry. The most significant deviation involves the $\text{Br}(3)\text{-Sb-Br}(3)'$ angle which is $177.0(3)^\circ$. This slight distortion can be ascribed to packing effects since the closest approach between anions is $3.584(5)\text{\AA}$ along the \underline{a} direction ($\text{Br}(3)\text{---}\text{Br}(3)''$) which is significantly shorter than the 3.9\AA sum of the van der Waals radii.²⁵ The average Sb-Br bond length is $2.549(5)\text{\AA}$ before correction for thermal motion and $2.565(5)\text{\AA}$ when corrected assuming a riding model. These averages are in good agreement with those previously reported.⁷ The tetraethylammonium ion has the trans configuration in which the ethyl groups lie on intersecting mirror planes (C_{2v} symmetry) as required by this space group. However, the inner carbon atoms do not lie on the mirror planes and are therefore disordered with apparent D_{2h} symmetry, as shown in Figure 4. Disorder within the swastika configuration of the tetraethylammonium ion has also been reported.²⁶ The long bond lengths indicate that the light atom positions are not well defined and reflect both the disorder and the heavy atom nature of this problem.

The crystal structure (Figure 3) can be viewed as an efficient packing arrangement of the rather spherical hexabromoantimonate(V) anions and of the somewhat equal size but slightly flattened tetraethylammonium cations. The similar sizes of these two large, rather diffuse ions contribute to crystal stability. The usual type of intervalence charge

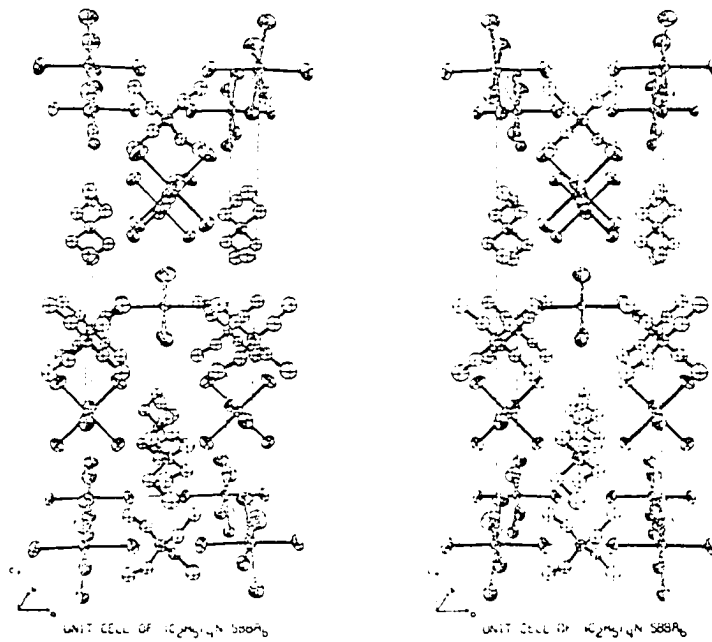


Figure 3. Stereogram of the unit cell showing packing of the $(C_2H_5)_4NSbBr_6$ units; the hydrogens are not shown

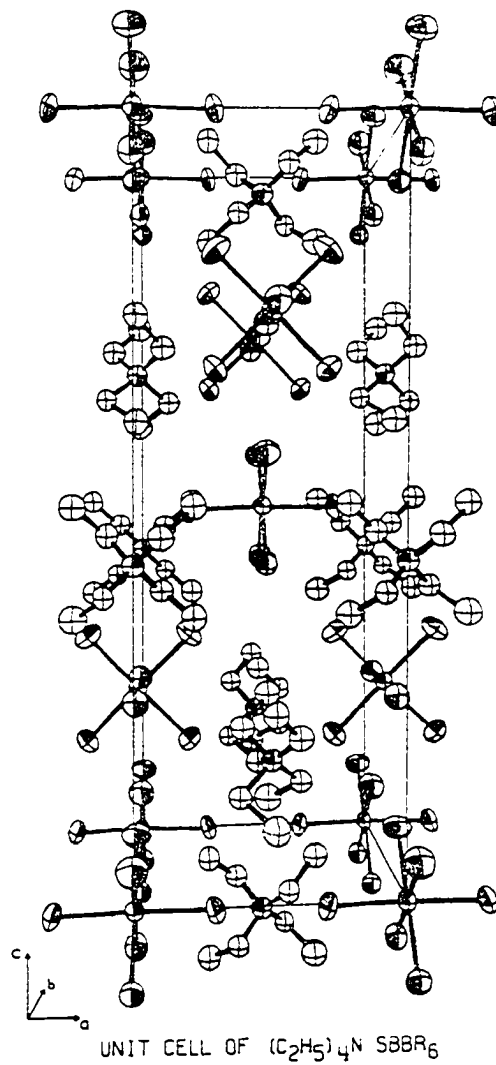
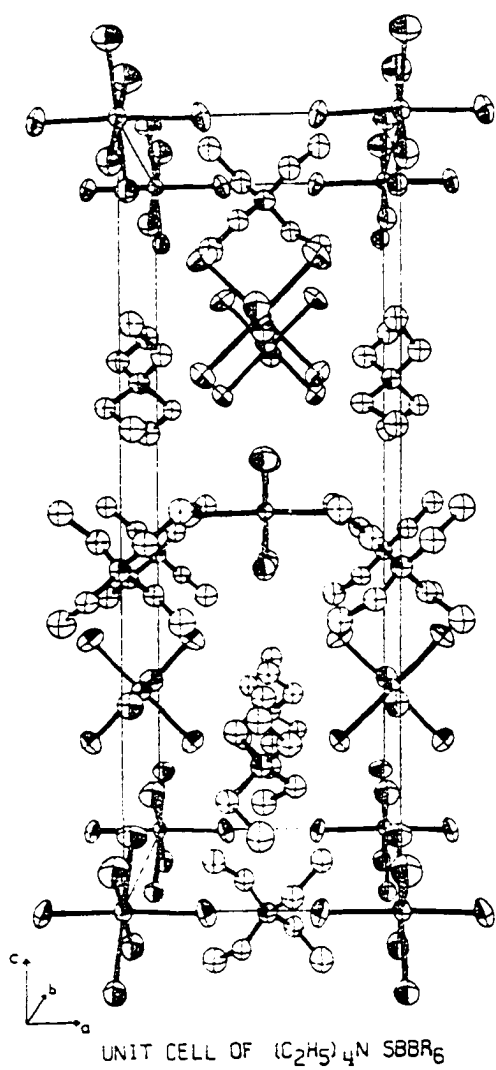


Figure 3 (continued) Cross eyes to view stereogram

Table 2. Selected interatomic bond distances and angles for $(C_2H_5)_4NSbBr_6^a$

Atoms	Distance(Å)	Atoms	Angle(°)
Sb-Br(1)	2.536(5)	Br(1)-Sb-Br(1)'	88.5(3)
Sb-Br(2)	2.553(5)	Br(1)-Sb-Br(2)'	91.2(1)
Sb-Br(3)	2.559(4)	Br(1)-Sb-Br(3)	91.1(1)
Br(1)-Br(1)'	3.540(12)	Br(2)-Sb-Br(2)'	89.0(3)
Br(1)-Br(2)''	3.636(5)	Br(2)-Sb-Br(3)	88.9(1)
Br(1)-Br(3)	3.636(5)	Br(1)-Sb-Br(2)	179.8(5)
Br(2)-Br(2)'	3.579(10)	Br(3)-Sb-Br(3)'	177.0(3)
Br(2)-Br(3)	3.581(5)		
Br(3)-Br(3) _i '	3.584(5)	C(3)-N-C(4)	112(3)
Br(1)-Br(2) _{ii} '	4.053(6)	C(3)-N-C(4)''	105(3)
N-C(3)	1.62(5)	C(3)-N-C(3)''	113(4)
N-C(4)	1.51(5)	C(3)''-N-C(4)	105(3)
C(3)-C(1)	1.63(6)	C(4)-N-C(4)''	109(5)
C(4)-C(2)	1.64(7)	N-C(3)-C(1)	101(3)
		N-C(4)-C(2)	113(4)
Atoms	Distance(Å) ^b		
Sb-Br(1)	2.561(5)		
Sb-Br(2)	2.564(5)		
Sb-Br(3)	2.570(4)		

^aPrimed atoms refer to the symmetry related atom in the group (Figure 4). Other symmetry operations referred to are:

- i) $1 + x, y, z$ ii) $x, 1/2 + y, 1/4 + z$.

^bInteratomic distance corrected for thermal motion using a riding model where second atom is assumed to ride on first.

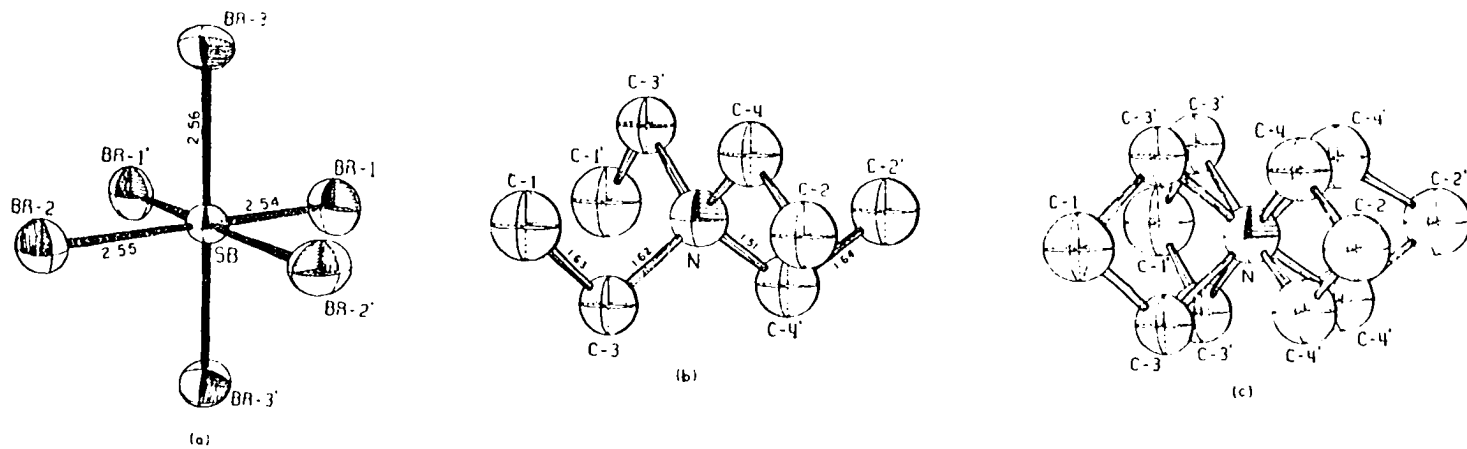


Figure 4. Ions present in $(C_2H_5)_4NSbBr_6$: a) $SbBr_6^-$; b) $(C_2H_5)_4N^+$; and c) disordered form of $(C_2H_5)_4N^+$

transfer cannot occur in this structure. The structure consists of only one kind of SbBr_6 species, has a saturated cation, and has only the one bromine---bromine contact ($\text{Br}(3)\text{---Br}(3)_i$, 3.58\AA) which is less than the sum of the van der Waals radii. This distance does not appear to be short enough to account for any type of interspecies charge transfer interaction since the $\text{Br}(3)\text{---Br}(2)$ and $\text{Br}(3)\text{---Br}(1)$ intra-ion distances are 3.58 and 3.64\AA , respectively. Therefore, the intense color of this complex probably results from normal charge transfer of the intraspecies ligand-to-metal type, involving transitions between molecular orbitals of the $\text{Sb}^{\text{V}}\text{Br}_6$ species.

THE STRUCTURE OF 4-ETHYLPYRIDINIUM TETRABROMOFERRATE(III)

Introduction

The crystal structure study of 4-ethylpyridinium tetrabromoferrate(III) was undertaken after it accidentally appeared as a byproduct during a series of investigations of bromo-coordinated antimony compounds being performed in this laboratory. The true composition was determined from the crystal structure analysis and also by an electron microprobe analysis of the crystal used in data collection. The crystal structure analysis of the tetrabromoferrate(III) compound was completed because of the general instability of iron(III) bromides and the lack of crystal structure data regarding the FeBr_4^- group.

Experimental

Crystal data:

4-Ethylpyridinium tetrabromoferrate(III), $\text{C}_7\text{H}_9\text{NHF eBr}_4$.

$M = 483.65$, Monoclinic $P2_1/c$, $F(000) = 900e$, $Z = 4$,

$a = 7.7068(8)$, $b = 14.1673(11)$, $c = 13.0414(16)\text{\AA}$, $\beta = 84.19(1)^\circ$,

$V = 1416.6\text{\AA}^3$, $D_c = 2.27\text{ g/cc}$, Mo K α ($\lambda = 0.7107\text{\AA}$), $\mu = 135.8\text{ cm}^{-1}$.

Single crystals of $\text{C}_7\text{H}_9\text{NHF eBr}_4$ were obtained accidentally from contamination introduced into a vessel where the corresponding antimony bromide salt was being prepared. Of the two crystalline forms present, crystals of what later were determined to be the tetrabromoferrate(III) salt were selected because its crystal habit was more suitable for X-ray

analysis, the other crystals having one very short dimension. The true composition was later determined from the crystal structure analysis and an electron microprobe analysis.

The compound has subsequently been prepared by adding 4-ethylpyridine to a solution of iron and Br_2 dissolved in hot concentrated hydrobromic acid. In this preparation a deep red-black crystalline solid forms very slowly upon cooling. (An alternate preparation of similar tetrahaloferrate ions has been reported by Clausen and Good.²⁷) Precession photographs of these crystals are identical to those obtained from the crystal used in data collection. These photographs exhibited 2/m Laue symmetry with the following systematic absences: $0k0$ when $k = 2n + 1$ and $h0l$ when $l = 2n + 1$. These extinctions uniquely specify the monoclinic space group $P2_1/c$. The unit cell parameters and their standard deviations were obtained by a least-squares fit¹³ to 13 independent reflection angles whose centers were obtained by careful alignment of the crystal on a General Electric single crystal orienter using a 1° take-off angle and Cr $K\alpha_1$ radiation ($\lambda = 2.28962\text{\AA}$).

A crystal of approximate dimensions $0.14 \times 0.15 \times 0.35$ mm was mounted in a 0.2 mm thin-walled Lindemann glass capillary with the c axis (0.35 mm) parallel to the phi axis and used for data collection. Data were taken at room temperature ($T \approx 24^\circ$) utilizing a fully automated Hilger-Watts four circle diffractometer equipped with scintillation counter. Mo $K\alpha$ ($\lambda = 0.7107\text{\AA}$) radiation was used with balanced (Zr-Y) filters to obtain intensity and individual background readings. The θ - 2θ step scan technique with a 4.5° take-off angle was used to record 1751 reflections within a 2θ sphere of 50° ($\sin\theta/\lambda = 0.595\text{\AA}^{-1}$). A variable

scan range was employed of 50 steps plus 2 per deg θ at a counting rate of 0.2048 sec per step of 0.01 deg in θ . As a general check on electronic and crystal stability, the intensities of three standard reflections were remeasured periodically during the data collection. Comparison of these values indicated that no decomposition had occurred.

The intensity data were also corrected for Lorentz-polarization effects and for effects due to absorption ($\mu = 135.8 \text{ cm}^{-1}$). The absorption correction¹⁵ was made using the program ABCOR¹⁶; the maximum and minimum transmission factors were 0.215 and 0.196, respectively. The estimated error in each intensity measurement was calculated by

$$\overline{\sigma(I)}^2 = \overline{C_T + C_B + (0.05C_T)^2 + (0.10C_B)^2 + (0.05C_R)^2} / A^2$$

where C_T , C_B , C_R and A are the total count, background count, net count and the transmission factor, respectively. The estimated standard deviation of each structure factor was calculated from the estimated errors in the intensity using the method of finite differences of Williams and Rundle.¹⁷ The reciprocals of the structure factor variances were used as the weights during the refinement. Based on the measurement of symmetry extinct reflections, it was decided that only those reflections for which $I > 3\sigma(I)$ would be considered observed. The results reported below are based on the 762 remaining observed reflections.

Solution and Refinement

The observed Patterson was difficult to interpret because of preconceived notions regarding the distances and geometry expected for antimony-bromide polyhedra. A series of single superpositions²⁸⁻³⁰ was

then carried out³¹ using general peaks on a sharpened Patterson.³² (An example of the Patterson superposition technique is given in Figure 5.) Comparison of the resulting maps revealed an MX_4 heavy atom group of tetrahedral geometry. These coordinates were input as an SbBr_4 group with fixed thermal parameters and refined by a full matrix least-squares procedure minimizing the function $\sum w(|F_o| - |F_c|)^2$. Examination of the resulting electron density map revealed all non-hydrogen atom positions. Isotropic refinement resulted in a conventional R factor ($R = (\sum(|F_o| - |F_c|))/\sum|F_o|$) of 0.185 and a weighted R factor $R_w = (\sum w(|F_o| - |F_c|)^2/\sum w|F_o|^2)^{\frac{1}{2}}$ of 0.223.

The multiplier of the metal atom was next allowed to vary while the scale and its thermal parameters remained fixed. The multiplier varied from 1.00 to 0.53, lowering the discrepancy factor to $R = 0.156$. This implied that the central metal atom was smaller than an antimony, atomic number ≈ 27 , in agreement with the shorter M-Br distances found. An electron microprobe analysis of the crystal used for data collection confirmed the absence of antimony and indicated the presence of iron and bromine. Preliminary treatment of the data was then repeated as described earlier using the new absorption coefficient. Subsequent refinement based on FeBr_4 proceeded smoothly, and with anisotropic thermal parameters for all non-hydrogen atoms converged to a discrepancy factor of $R = 0.056$ and $R_w = 0.089$.

Unusually large thermal ellipsoids were obtained for the ethyl carbons, and a least-squares plane analysis of the pyridinium ring atoms revealed deviations as large as 0.05\AA . It was therefore decided to use rigid body refinement for the ring and adjacent atoms. The C-N bond

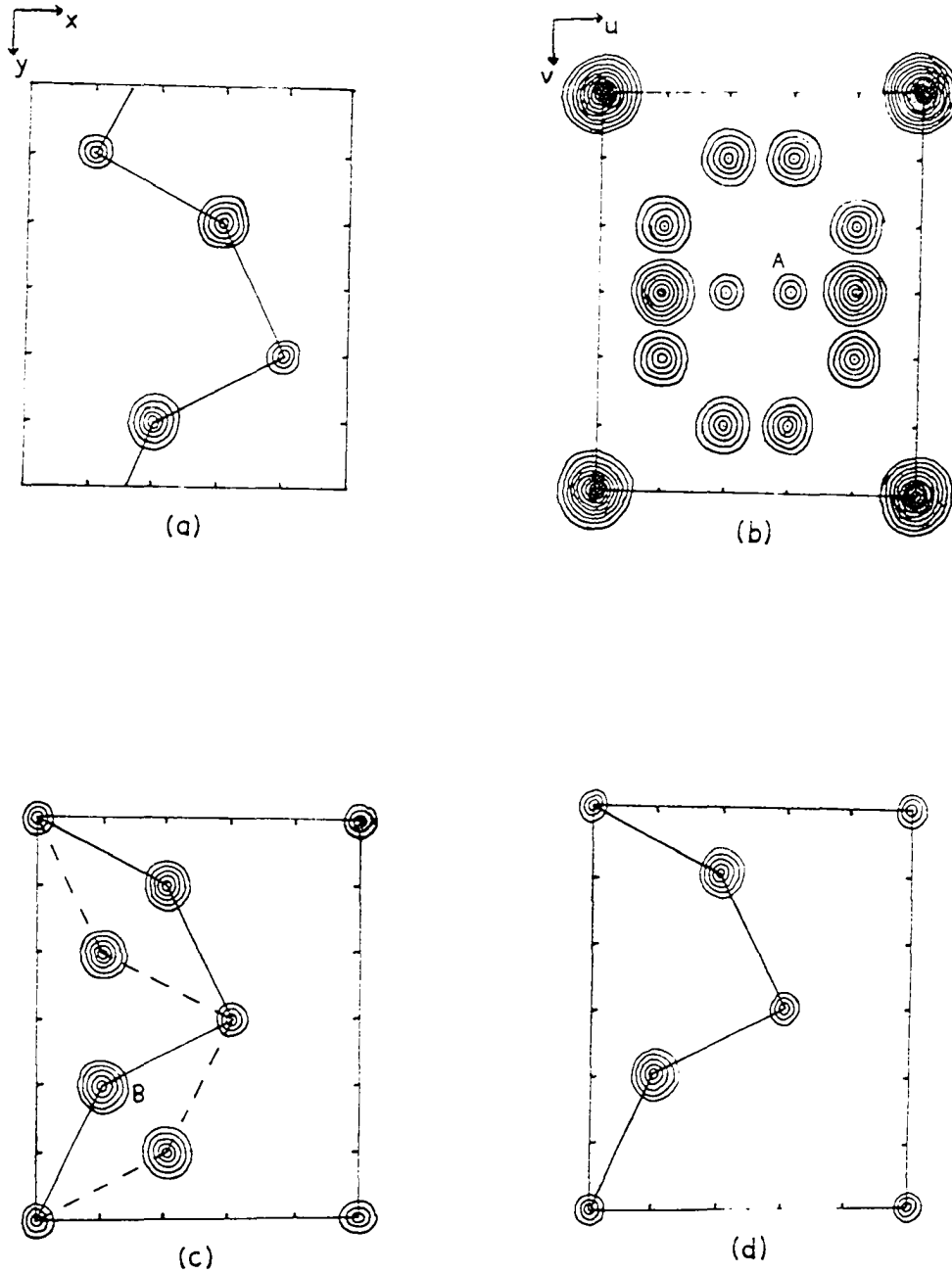


Figure 5. (a) Electron density map, (b) Patterson map, (c) Results of single superposition on peak A with structure and its inverse shown, and (d) Double superposition using peaks A and B yielding resultant structure

length was taken as 1.340\AA and the four C-C lengths as 1.394\AA each.³³ This decreased the number of variables from 118 to 62, and refinement converged to a discrepancy factor of $R = 0.061$ and a weighted discrepancy factor of $R_w = 0.096$. A final electron density difference map showed no peak heights greater than $0.4e/\text{\AA}^3$.

The relativistic Hartree-Fock X-ray scattering factors for neutral atoms of Doyle and Turner²¹ were used, with those of iron and bromine being modified for the real and imaginary parts of anomalous dispersion.²² The scattering factor used for hydrogen was the contracted form of Stewart, Davidson, and Simpson.³⁴ Based on the agreement of the large structure factors, no extinction correction was necessary. The final positional and thermal parameters and their standard errors as derived from the inverse matrix of the final least-squares cycle are given in Table 3. Positional coordinates of the group atoms are listed in Table 4. The final values of the observed and calculated structure factors ($x10$) are listed in Figure 6.

Description of the Structure

The tetrabromoferrate(III) group describes a slightly distorted tetrahedron with bond distances ranging from 2.309 to 2.345\AA and bond angles of 107.7 to 110.9° , the averages being 2.326\AA and 109.5° . This average Fe-Br distance becomes 2.347\AA (range 2.328 to 2.362\AA) when the interatomic distances are corrected for thermal motion, using a riding model approximation. The shortest bromine---bromine contact within the group is 3.76\AA . All bond distances and angles of interest are listed in

Table 3. Final positional and thermal parameters for $C_7H_9NHFeBr_4$ ^a

Atom	x	y	z	β_{11}	β_{22}	β_{33}	β_{12}	β_{13}	β_{23}
Fe	0.3045(4)	0.2603(2)	0.0646(3)	181(7)	61(2)	59(3)	2(3)	-20(3)	3(2)
Br(1)	0.3562(4)	0.1058(2)	0.0138(2)	363(8)	60(2)	92(3)	21(3)	-13(4)	-3(2)
Br(2)	0.0310(4)	0.3096(3)	0.0259(2)	222(7)	123(3)	97(3)	56(3)	-33(3)	-5(2)
Br(3)	0.5212(4)	0.3567(3)	-0.0163(3)	317(8)	108(3)	92(3)	-66(4)	-6(4)	13(2)
Br(4)	0.3148(4)	0.2673(2)	0.2435(2)	304(7)	103(2)	52(2)	-24(3)	-18(3)	-3(2)
C(8)	1.1980(60)	0.6012(49)	0.3054(37)	568(148)	443(89)	200(57)	-217(97)	-132(70)	-160(60)

^aStandard errors of the coordinates and the β_{ij} and their standard errors are $\times 10^4$. The β_{ij} are defined by:

$$T = \exp[-(h^2 \beta_{11} + k^2 \beta_{22} + l^2 \beta_{33} + 2hk \beta_{12} + 2hl \beta_{13} + 2kl \beta_{23})].$$

Table 4. Group parameters for $C_7H_9NHFeBr_4$ ^a

$x_o = 0.6708(21)$		$\rho = 8.91(35)$
$y_o = 0.3869(13)$		$\theta = -45.63(83)$
$z_o = 0.2868(15)$		$\varphi = 39.77(86)$
$\text{Group B} = 3.96(35)\text{\AA}^2$		

Atom	x	y	z
N(1)	0.6708	0.3869	0.2868
C(2)	0.6928	0.4563	0.2168
C(3)	0.8419	0.5123	0.2023
C(4)	0.9764	0.4957	0.2638
C(5)	0.9557	0.4239	0.3369
C(6)	0.8013	0.3719	0.3453
C(7)	1.1442	0.5555	0.2512
H(1)	0.5564	0.3462	0.2953
H(2)	0.5897	0.4700	0.1685
H(3)	0.8530	0.5674	0.1447
H(5)	1.0569	0.4088	0.3861
H(6)	0.7872	0.3164	0.4023

^aThe group was defined in the xy plane of the orthogonal coordinate system with the two fold axis along x; x_o , y_o and z_o refer to the group origin and ρ , θ and φ are the rotation angles in degrees as defined by Scheringer.³⁵

The fixed individual thermal parameters assigned group atoms were 3.5, 8.5 and 6.0\AA^2 for the ring atoms, C(7) and hydrogens, respectively.

Table 5 (also see Figure 7). The ring atoms of the 4-ethylpyridinium cation were fixed in the rigid body refinement. The unusually short C(7)-C(8) distance obtained in the ethyl group is a result of the large thermal parameters associated with those atoms. Using the anisotropic thermal parameters obtained from the earlier refinement, this distance adjusts to 1.51\AA when a riding model is assumed. The high thermal motion of the cation can be attributed to the size of its cavity.

A unit cell drawing of 4-ethylpyridinium tetrabromoferrate(III) is shown in Figure 8. The FeBr_4 tetrahedra are nearly aligned with their three-fold axes almost coincident in the c direction. The closest bromine---bromine distance in this direction is 4.00\AA , which is greater than the sum of the van der Waals radii of 3.90\AA .²⁵ The shortest interatomic bromine---bromine distance is 3.72\AA involving Br(1) across a center of symmetry. One significantly short hydrogen---bromine distance involving H(1) and Br(4) of 2.3\AA is present. The Fe-Br(4)---H(1) and Br(4)---H(1)-N(1) angles are 115 and 157° , respectively. The Fe-Br(4) bond distance is also slightly longer than the other Fe-Br distances. This N-H---Br(4) hydrogen bond^{36,37} may contribute to the slight ion deformation and the crystal stability of this compound.

Table 5. Interatomic distances and angles in $C_7H_9NHFeBr_4$ ^a

a) $FeBr_4$ anion				
	d(Å)	d _{corr.}	angle	(°)
Fe-Br(1)	2.309(4)	2.328(4)	Br(1)-Fe-Br(2)	110.9(2)
Fe-Br(2)	2.324(4)	2.347(4)	Br(1)-Fe-Br(3)	109.3(2)
Fe-Br(3)	2.326(4)	2.351(4)	Br(1)-Fe-Br(4)	107.7(2)
Fe-Br(4)	2.345(4)	2.362(4)	Br(2)-Fe-Br(3)	110.5(2)
Br(1)-Br(4)	3.757(4)	--	Br(2)-Fe-Br(4)	109.0(2)
Br(2)-Br(3)	3.821(4)	--	Br(3)-Fe-Br(4)	109.4(2)
b) $C_7H_9NH^+$ cation				
C-N	1.340		C(6)-N(1)-C(2)	117.0
C-C	1.394		N(1)-C(2)-C(3)	123.7
N-H	1.050		N(1)-C(6)-C(5)	123.7
C-H	1.080		C(2)-C(3)-C(4)	118.5
C(4)-C(7)	1.540		C(6)-C(5)-C(4)	118.5
C(7)-C(8)	1.073		C(3)-C(4)-C(5)	118.5
			C(4)-C(7)-C(8)	129.6
c) Other				
Br(4)--H(1)	2.330		Br(4)-H(1)-N(1)	156.9
Br(4)--N(1)	3.321		Fe-Br(4)-H(1)	114.7
Br(1)--Br(1) _i	3.724(5)		Fe-Br(4)-N(1)	107.6
Br(4)--Br(1) _{ii}	3.998(4)			

^aSymmetry operations referred to are:

i) $\bar{x}, \bar{y}, \bar{z}$

ii) $x, 1/2 - y, 1/2 + z.$

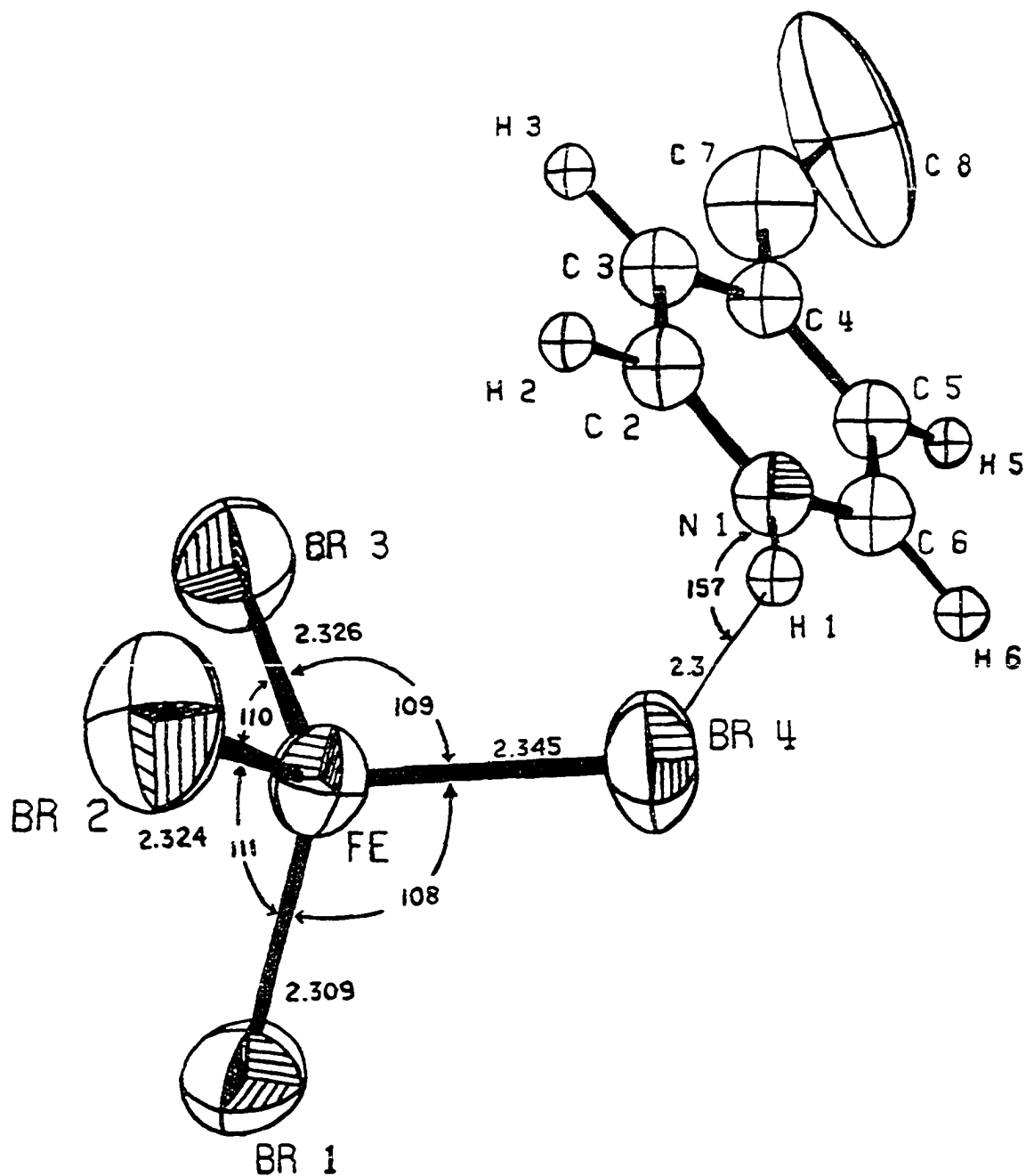


Figure 7. A formula unit of 4-ethylpyridinium tetrabromoferrate(III) showing presence of N-H...Br hydrogen bond

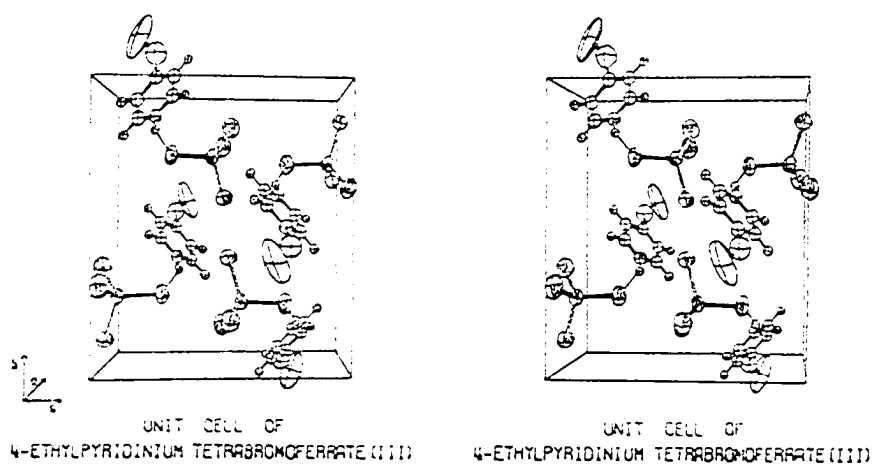
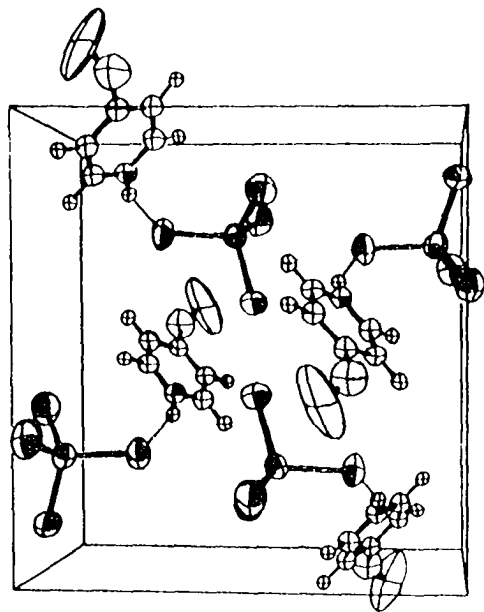
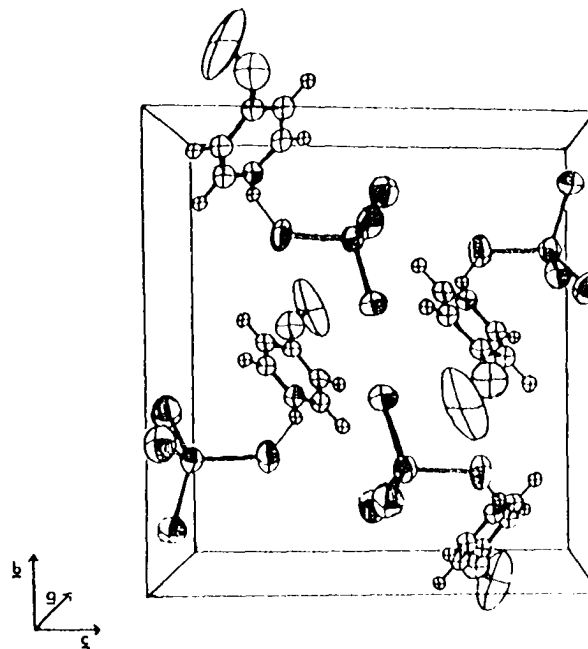


Figure 8. Stereogram of unit cell showing packing of 4-ethylpyridinium tetrabromoferrate(III) units



UNIT CELL OF
4-ETHYLPYRIDINIUM TETRABROMOFERRATE (III)



UNIT CELL OF
4-ETHYLPYRIDINIUM TETRABROMOFERRATE (III)

Figure 8 (continued) Cross eyes to view stereogram

THE CRYSTAL AND MOLECULAR STRUCTURE OF D-GLUCONO-(1,5)-LACTONE

Introduction

An accurate structural investigation of D-glucono-(1,5)-lactone was undertaken because aldonolactones are inhibitors of glycosidases and other enzymes of carbohydrate metabolism. All non-hydrogen positions were determined by aid of a symmetry map used in conjunction with the Patterson superposition technique. This method is illustrated in Figure 9. We feel that this method, or a modification of it, is generally applicable for moderately sized molecules.

Experimental

Crystal data:

$C_6H_{10}O_6$, $M = 178.14$, Orthorhombic $P2_12_12_1$,
 $a = 7.838(1)$, $b = 12.332(2)$, and $c = 7.544(1)\text{\AA}$,
 $V = 729.2\text{\AA}^3$, $D_c = 1.62\text{g/cc}$, $Z = 4$, $F(000) = 376$,
 $Mo\ K\alpha(\lambda = 0.7107\text{\AA})$, $\mu = 1.60\text{ cm}^{-1}$.

Suitable crystals were obtained by recrystallizing commercially available glucono- δ -lactone from a saturated DMF (dimethylformamide) solution allowed to evaporate slowly. The colorless crystals grew with b perpendicular to and a and c along the diagonals of the broad face. Precession and Weissenberg photographs exhibited mmm Laue symmetry with alternate extinctions along the axes indicating the orthorhombic space group $P2_12_12_1$. The unit cell parameters and their standard deviations

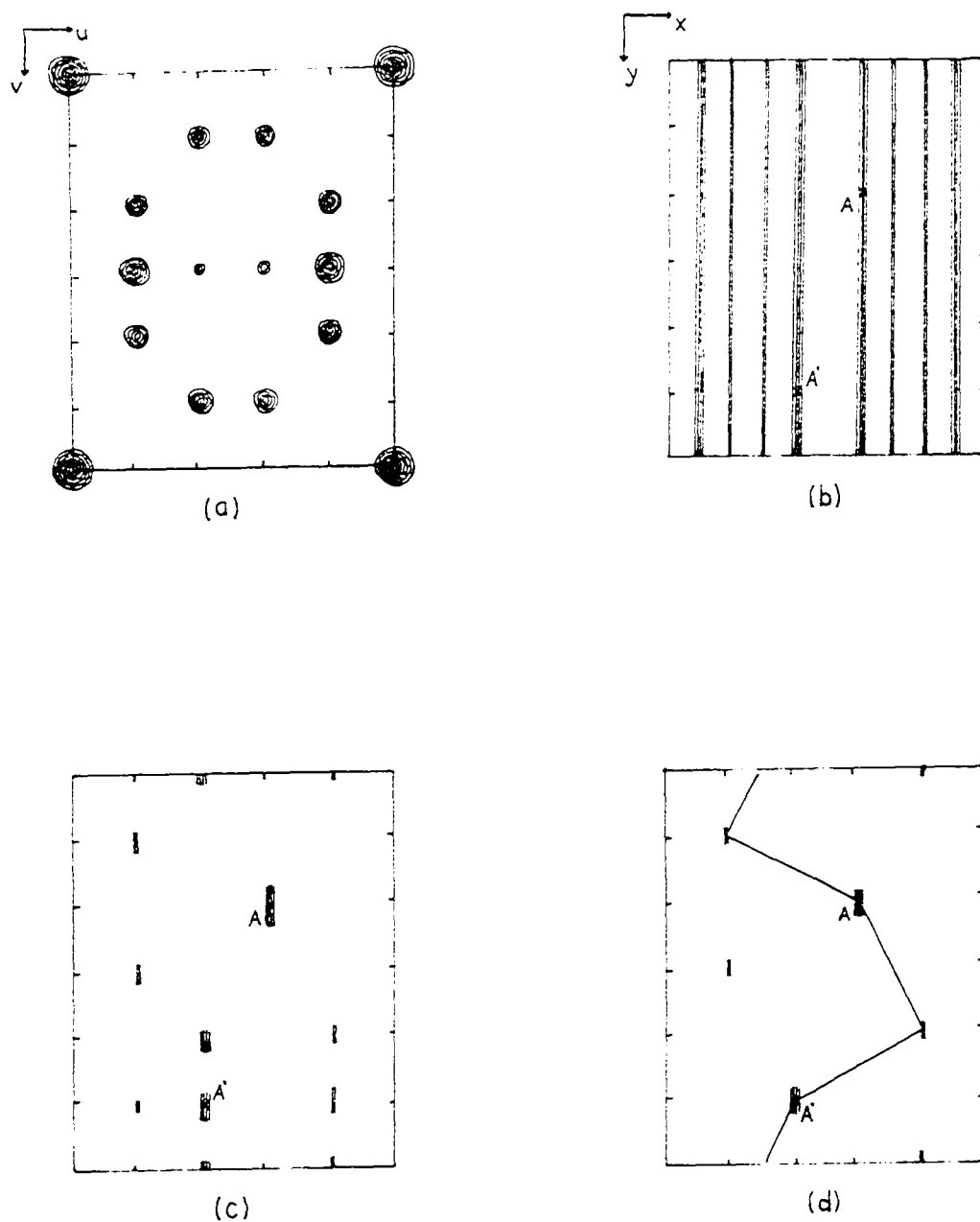


Figure 9. (a) Patterson map, (b) Symmetry map computed from Harker plane at $v = 1/2$, (c) Intermediate superposition results using only peak A of symmetry related pair (A,A'), and (d) Results of two superpositions using peaks A and A'

were obtained by a least-squares fit¹³ to 14 independent reflection angles whose centers were determined by left-right, top-bottom beam splitting on a previously aligned Hilger-Watts four-circle diffractometer (Mo K α radiation). Any error in the instrumental zero was eliminated by centering the reflection at both $+2\theta$ and -2θ .

A crystal of dimensions 0.24 x 0.20 x 0.12 mm was mounted on a glass fiber with b along the spindle axis for data collection. Intensity data were taken at room temperature (24°C) using a fully automated Hilger-Watts four-circle diffractometer equipped with scintillation counter and interfaced with an SDS-910 computer in a real time mode. Two equivalent octants of data were taken using Zr-filtered Mo K α radiation within a θ sphere of 35° ($\sin\theta/\lambda = 0.8071$). The θ - 2θ step-scan technique, 0.01°/step counting for 0.4096 sec/step, was employed with a take-off angle of 4.5°. To improve the efficiency of the data collection process, variable step symmetric scan ranges were used. The number of steps used for a particular reflection was 50 + 2 per degree θ . Individual backgrounds were obtained from stationary crystal-stationary counter measurements for one-half the total scan time at each end of the scan.

The intensities of three standard reflections were measured periodically during the data collection. Monitoring options based on these standard counts were employed to maintain crystal alignment and to stop the data collection process if the standard counts fell below statistically allowed fluctuations. A total of 3762 reflections were recorded in this manner.

The intensity data were corrected for Lorentz-polarization effects. Because of the small linear absorption coefficient, no absorption

correction was made. The minimum and maximum transmission factors were 0.96 and 0.98, respectively. Because absorption was negligible, the consistency of equivalent data was easily checked. Those equivalent reflections differing by more than $5\sigma = 5\sqrt{C_T}$ were retaken. This affected some 150 reflections. The individual values of F_o^2 from the equivalent octants were then averaged to yield 1851 independent F_o^2 values. Standard deviations in the intensities were estimated from the average total counts and background values by

$$\overline{[\sigma(I)]^2} = C_T + C_B + (0.05 * C_T)^2 + (0.05 * C_B)^2.$$

Of the 1851 independent reflections, 974 had $F_o^2 > 2.5 * \sigma(I)$. These were used in the initial stages of refinement. The estimated standard deviation in each structure factor was calculated from the mean deviation in intensity by the method of finite differences.¹⁷ The reciprocals of the structure factor variances were used as weights in the least squares refinement. When all atom positions were located, final weighted least-squares refinement was completed using all of the independent reflection data.

Solution and Refinement

The observed data were used to compute an unsharpened Patterson map. The resulting map contained many broad, overlapping peaks which made it unsuitable for superposition techniques. To reduce the peak width, sharpened coefficients³² were computed by

$$|F_{hkl}^s|^2 = [|F_{hkl}^o| / (\hat{f}k)]^2 \exp [(2B - B') \sin^2 \theta / \lambda^2]$$

where $\hat{f} = \sum f_j / \sum_j$, k is a scale factor, B is the overall isotropic temperature factor, and B' is a variable used to minimize rippling resulting

from sharpening. Estimates of the overall temperature and scale factors were obtained from a Wilson plot.³⁸ A sharpened Patterson map of good resolution was obtained using $2B-B' = 2.0\text{\AA}^2$.

Examination of the sharpened Patterson map, and initial superposition²⁸⁻³¹ attempts produced no realistic model; therefore a symmetry map³⁹⁻⁴³ was next calculated. Peaks only occur on the symmetry map at those electron density positions which are consistent with the Harker peaks⁴⁴ of the Patterson map. The value assigned to each point of the symmetry map was obtained by taking the minimum of the values of the associated points on the three Harker planes. In order that no information on these planes be discarded, the maximum value at the point and the four other points immediately surrounding it in the plane was taken before carrying out the minimum procedure. A section of the symmetry map computed in this way is shown in Figure 10. Since no origin has been specified, not 1 but 64 images of the unit cell appear on this map due to the orthorhombic symmetry. However, to isolate one image, it is possible to select a peak from the symmetry map and superimpose the sharpened Patterson on this and its symmetry related points. This procedure is just one of the superposition techniques possible using a symmetry map. After a couple of unpromising choices, a single peak was selected and a set of four symmetry map--Patterson map superpositions was carried out (Figure 11). Analysis of the resulting map showed that there were only 32 consistent, independent peaks remaining. A second peak was chosen from what appeared to be the same image and another set of four such superpositions was carried out (Figure 12). Analyzing the resultant map

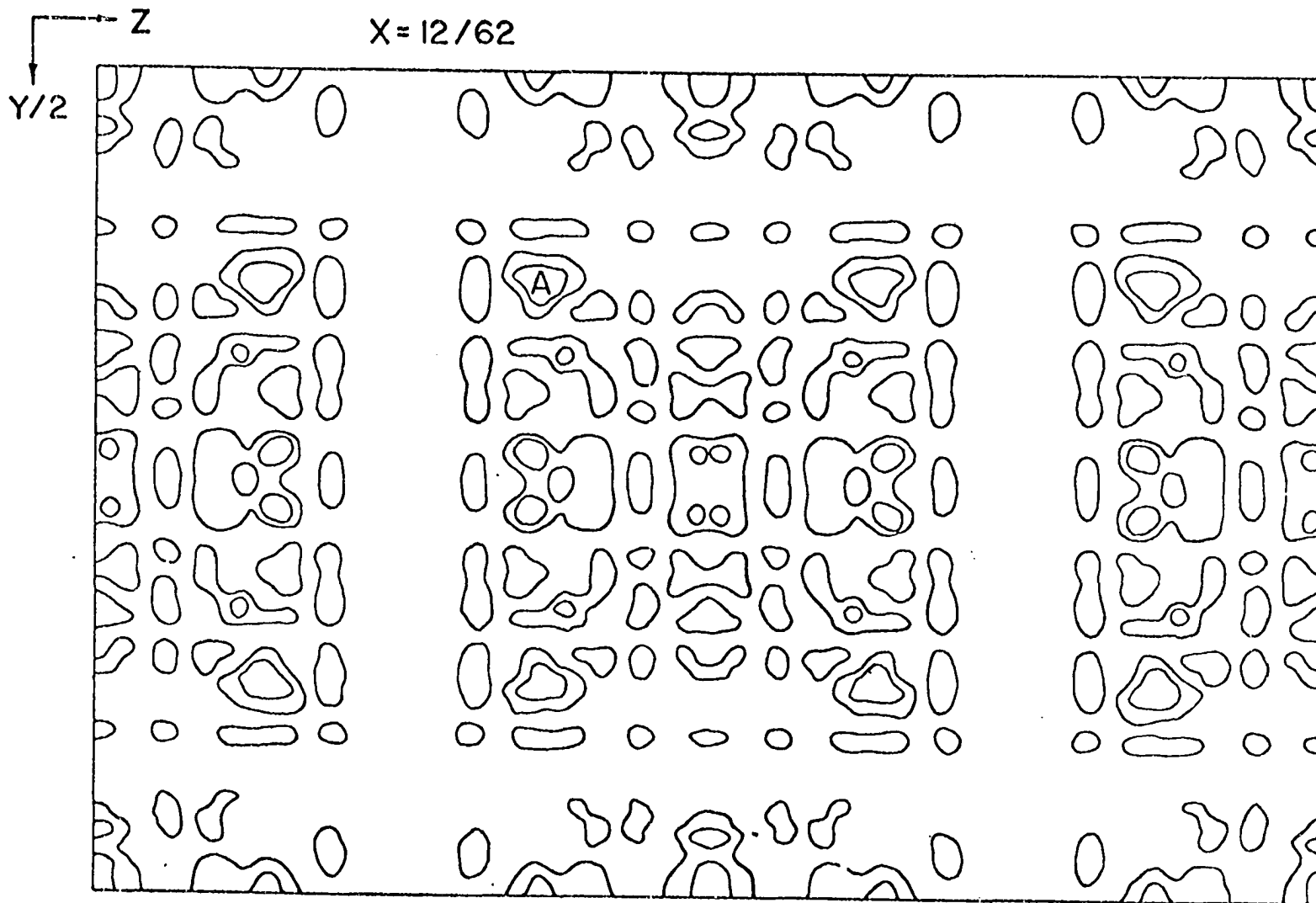


Figure 10. Section of the symmetry map computed for gluconolactone

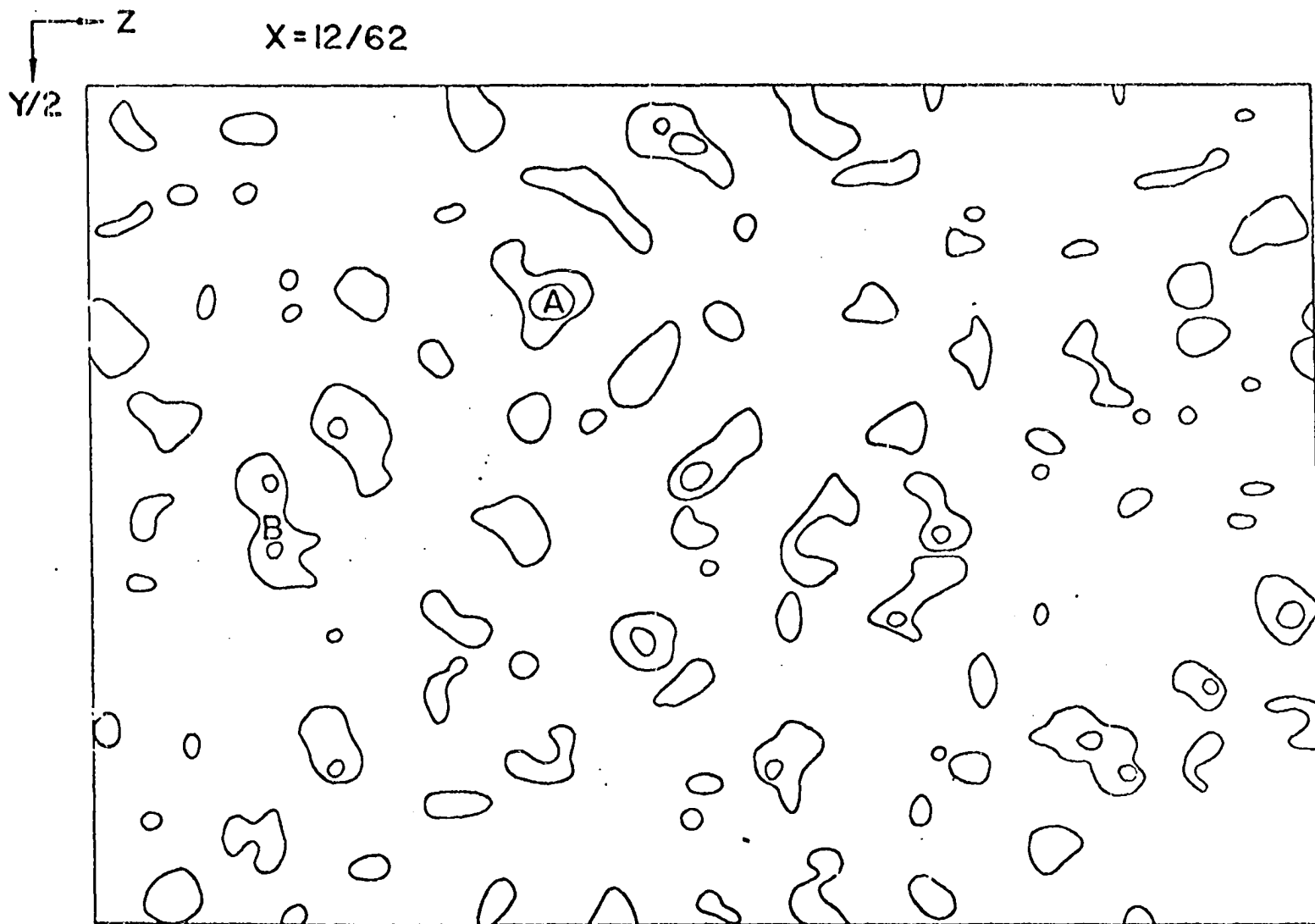


Figure 11. Section showing results of four superpositions on the symmetry map using the peak marked A (Figure 10) and its three related positions

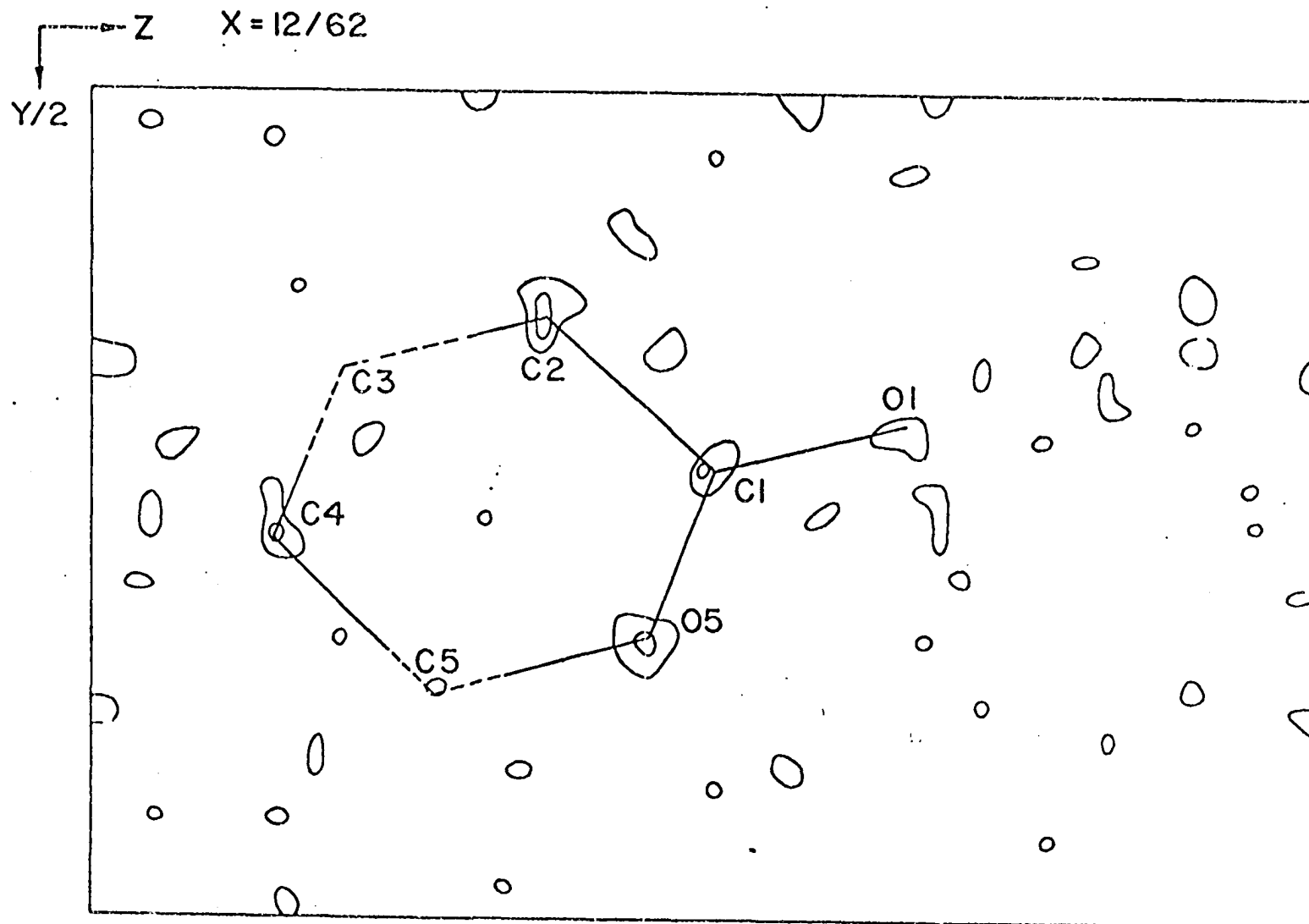


Figure 12. Section showing results of eight superpositions using peaks A and B (Figure 11) and their symmetry related positions

and correlating it with the first reduced the number of possible peak positions to 18 with a fragment of the molecule now readily observable. A third peak was chosen from the visible fragment and another set of superpositions made. Correlation of the three maps easily resolved the previous ambiguities, locating all carbon and oxygen positions.

Three cycles of full-matrix least-squares refinement of these heavy atom positional and isotropic thermal parameters gave a conventional discrepancy factor $R = \sum ||F_o| - |F_c|| / \sum |F_o| = 0.109$ and a weighted R-factor $R_w = \sqrt{\sum_w (|F_o| - |F_c|)^2 / \sum_w |F_o|^2} = 0.133$ for the 974 observed reflections. The scattering factors used for carbon and oxygen were those of Doyle and Turner.²¹ A difference electron density map at this stage showed that all the non-hydrogen atoms had been accounted for, but that some anisotropic motion was evident. Anisotropic refinement of all heavy atom positions for two additional cycles lowered the discrepancy factor to $R = 0.071$ and $R_w = 0.090$. The following difference electron density map clearly indicated the positions of all hydrogens bound to carbon. These positions were input lowering the agreement factor to 0.057, but some of the isotropic thermal parameters went negative. This was attributed to the use of the isolated hydrogen atom scattering factor, leading to an undesirable interaction between the thermal parameter and the aspherical electron density distribution for bound hydrogen, as described by Jensen and Sundaralingam.⁴⁵ Using the contracted hydrogen atom scattering factor of Stewart, Davidson and Simpson,³⁴ positive isotropic thermal parameters were derived. All remaining hydrogen atom positions were obtained from subsequent difference electron density maps. Final values of R and R_w of 0.046 and 0.051, respectively, were obtained for the 974 observed

reflections. At this point two final cycles of weighted least-squares refinement of all parameters were run using all 1851 independent reflections recorded, the results being $R = 0.095$ and $R_w = 0.049$. No appreciable shifts occurred. A final electron density difference map showed no peak heights greater than $0.3e/\text{\AA}^3$. A statistical analysis of $\omega\Delta^2$ [where $\Delta^2 = (|F_o| - |F_c|)^2$] as a function of scattering angle and magnitude of F_o yielded a nearly straight line indicating the relative weighting scheme used was reasonable. The final value of $[\sum\omega\Delta^2/(NO-NV)]^{\frac{1}{2}}$ was 1.11.

In Table 6 are listed the final positional and thermal parameters of the heavy atoms along with their standard deviations. In Table 7 are the refined positional and isotropic thermal parameters and their standard deviations for the hydrogen atoms. Standard deviations given were obtained from the inverse matrix of the final least-squares refinement cycle. A list of all 1851 independent recorded and calculated structure amplitudes ($\times 10$) is found in Figure 13. An indication of the directions and root-mean-square amplitudes of vibration for the non-hydrogen atoms is provided by Figure 14. The bond lengths and bond angles with standard deviations are given in Table 8 and Figure 15. The best least-squares plane through the δ -lactone carbonyl group was calculated from the final positional parameters. The equation of the least-squares plane and the displacement of the heavy atoms from this plane are given in Table 9.

Description of the Structure

The planarity of the carbonyl group imparts a distorted half-chair

Table 6. Final heavy atom atomic coordinates and thermal parameters for D-glucono-(1,5)-lactone^a

Atom	x	y	z	β_{11}	β_{22}	β_{33}	β_{12}	β_{13}	β_{23}
C(1)	0.2071(4)	0.2214(2)	0.4968(3)	99(4)	44(2)	74(4)	-4(2)	0(4)	3(2)
C(2)	0.1911(3)	0.1294(2)	0.6312(3)	82(4)	30(1)	86(4)	3(2)	2(4)	2(2)
C(3)	0.1067(3)	0.1632(2)	0.8022(3)	81(4)	36(1)	69(4)	6(2)	8(4)	9(2)
C(4)	0.1868(4)	0.2678(2)	0.8653(3)	96(4)	30(2)	67(4)	6(2)	1(3)	4(2)
C(5)	0.1586(4)	0.3581(2)	0.7304(3)	100(4)	36(1)	68(4)	7(2)	-0(4)	4(2)
C(6)	0.2550(3)	0.4599(2)	0.7670(4)	111(4)	33(2)	78(4)	-2(2)	-1(3)	-0(2)
O(1)	0.2238(3)	0.2023(2)	0.3407(2)	220(5)	56(2)	72(3)	-16(2)	16(3)	-0(2)
O(2)	0.1041(3)	0.0415(1)	0.5520(2)	122(4)	35(1)	118(3)	-3(2)	7(3)	-12(2)
O(3)	0.1304(3)	0.0782(2)	0.9267(3)	135(4)	38(1)	98(3)	15(2)	24(3)	22(2)
O(4)	0.1097(3)	0.3061(2)	1.0248(2)	192(5)	47(1)	71(3)	8(2)	19(3)	0(2)
O(5)	0.2100(3)	0.3233(1)	0.5521(2)	219(2)	37(1)	60(3)	-13(2)	8(3)	3(2)
O(6)	0.4331(3)	0.4429(2)	0.7852(3)	103(4)	69(2)	102(4)	-9(2)	-6(3)	9(2)

^aStandard errors of the coordinates and the β_{ij} and their standard errors are $\times 10^4$. The β_{ij} are defined by: $T = \exp[-(h^2\beta_{11} + k^2\beta_{22} + l^2\beta_{33} + 2hk\beta_{12} + 2hl\beta_{13} + 2kl\beta_{23})]$.

Table 7. Refined hydrogen atom parameters

Atom	x	y	z	B(\AA^2)
H(2)	0.308(3)	0.108(2)	0.654(3)	1.4(5)
H(3)	-0.013(3)	0.172(2)	0.785(3)	1.2(5)
H(4)	0.308(3)	0.261(2)	0.879(3)	2.1(6)
H(5)	0.044(3)	0.373(2)	0.728(4)	2.1(6)
H(6A)	0.218(4)	0.488(2)	0.877(4)	2.8(6)
H(6B)	0.235(3)	0.514(2)	0.680(3)	1.3(5)
H(2')	0.162(4)	-0.002(2)	0.509(4)	3.9(8)
H(3')	0.077(5)	0.089(3)	1.000(5)	5.0(10)
H(4')	0.147(4)	0.277(2)	1.100(4)	2.8(8)
H(6')	0.473(4)	0.433(3)	0.696(5)	4.2(9)

Figure 13 consists of a grid of 50 columns and 30 rows of data. Each cell in the grid contains a numerical value, likely representing structure factors. The values are arranged in a regular, repeating pattern across the entire grid. The numbers are printed in a monospaced font, typical of technical data sheets. The grid is composed of approximately 1500 individual numerical entries. The values vary in magnitude, with some appearing to be in the range of 0.1 to 1.0, and others appearing as small integers or fractions. The overall layout is that of a standard data table used for scientific or engineering purposes.

Figure 13. Observed and calculated structure factors (x10)

Table 8. Interatomic distances and angles^a in D-glucono-(1,5)-lactone

a) distances (Å) e.s.d. = 0.003Å			
C(1)-C(2)	1.527	C(1)-O(1)	1.208
C(2)-C(3)	1.508	C(1)-O(5)	1.324
C(3)-C(4)	1.512	C(2)-O(2)	1.414
C(4)-C(5)	1.525	C(3)-O(3)	1.419
C(5)-C(6)	1.491	C(4)-O(4)	1.427
		C(5)-O(5)	1.468
		C(6)-O(6)	1.418

b) angles (°) e.s.d. = 0.2°			
C(2)-C(1)-O(1)	120.7	C(3)-C(4)-C(5)	110.7
C(2)-C(1)-O(5)	119.8	C(3)-C(4)-O(4)	111.9
O(1)-C(1)-O(5)	119.4	C(5)-C(4)-O(4)	105.1
C(1)-C(2)-C(3)	113.5	C(4)-C(5)-C(6)	114.7
C(1)-C(2)-O(2)	109.2	C(4)-C(5)-O(5)	111.0
C(3)-C(2)-O(2)	111.2	C(6)-C(5)-O(5)	106.1
C(2)-C(3)-C(4)	108.8	C(5)-O(5)-C(1)	124.1
C(2)-C(3)-O(3)	107.8	C(5)-C(6)-O(6)	113.1
C(4)-C(3)-O(3)	111.5		

^aSee Figure 15 for distances and angles associated with hydrogen positions; e.s.d. are 0.03Å and 2°.

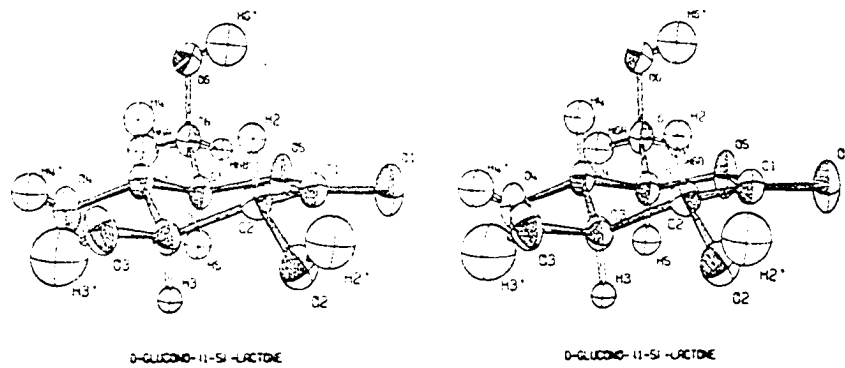
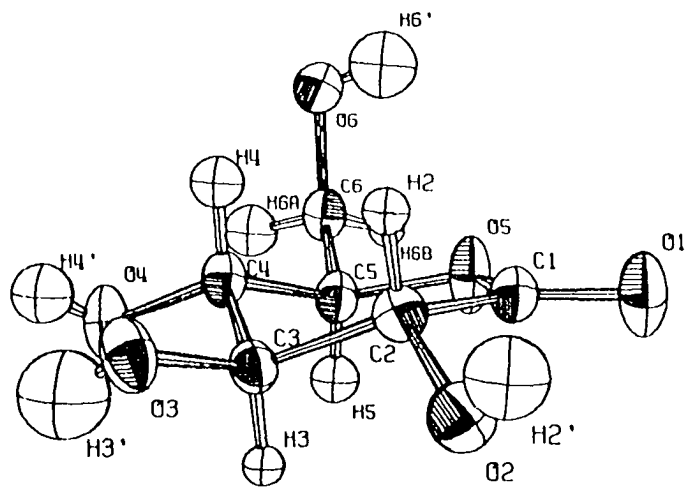
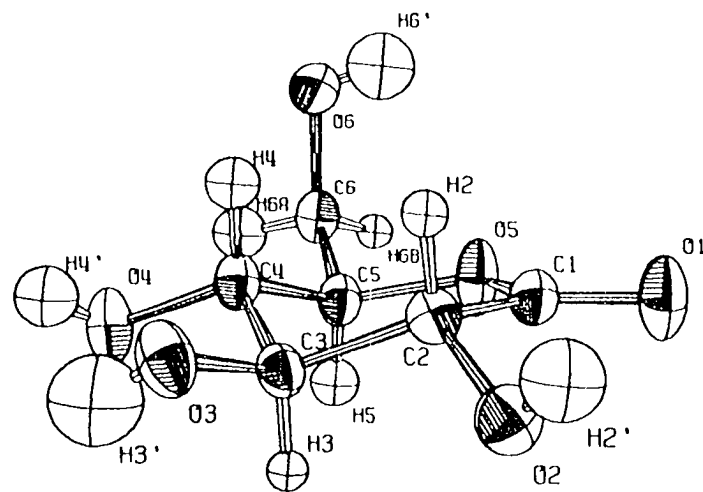


Figure 14. Stereogram of molecule with thermal ellipsoids scaled to enclose 50% probability



D-GLUCONO-(1-5)-LACTONE



D-GLUCONO-(1-5)-LACTONE

Figure 14 (continued) Cross eyes to view stereogram

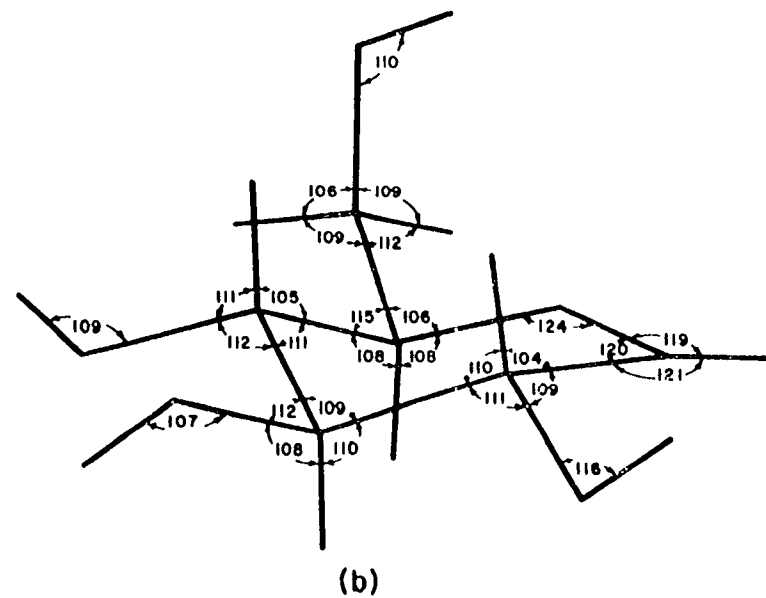
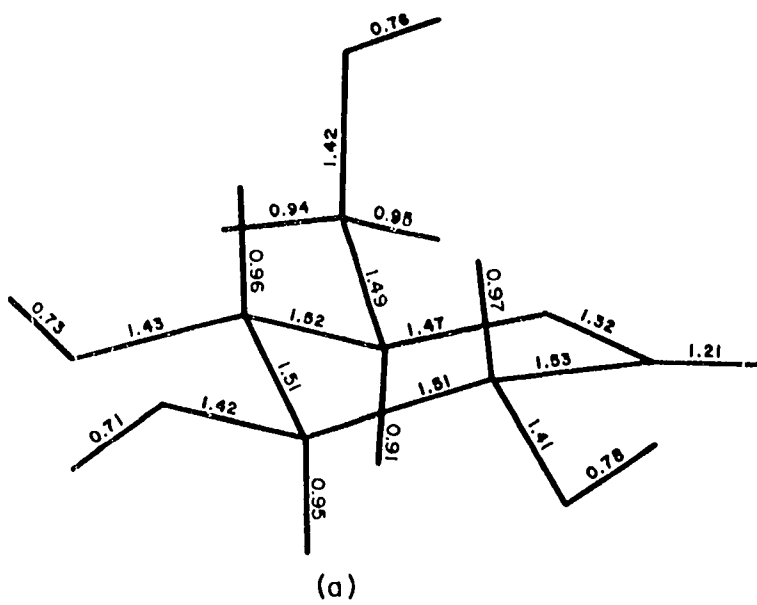


Figure 15. (a) Bond distances and (b) bond angles

Table 9. Least-squares plane

 Description (*)

C(1), C(2), O(1), O(5)

Equation relative to a, b, c

$$0.9941X - 0.0372Y + 0.1021Z - 1.910 = 0$$

Distance from plane (\AA)

C(1)*	-0.016	O(1)*	0.003
C(2)*	0.005	O(2)	-0.639
C(3)	-0.536	O(3)	-0.216
C(4)	0.088	O(4)	-0.408
C(5)	-0.277	O(5)*	0.003
C(6)	0.456	O(6)	1.865

conformation to the ring of the D-glucocno-(1,5)-lactone molecule. The CH_2OH and OH groups occupy the most equatorial positions possible as shown in Figure 14. The bond distances and angles are given in Table 8 and Figure 15 and in generally good agreement with those reported in the literature. The average C-C and C-OH distances are 1.51 and 1.42Å, respectively, compared to 1.52 and 1.42Å reported in the neutron diffraction study of α -D-glucose.⁴⁶ The C(5)-O(5) distance is significantly longer, however, being 1.47Å. The C(1)-O(1) and C(1)-O(5) distances are 1.21 and 1.32Å, typical of the distances found in normal esters. Peaks at 1740 and 1225 cm^{-1} in the infrared spectrum (Figure 16) substantiate this comparison. The angles about C(1) are all nearly 120° in accordance with the expected sp^2 hybridization. The only other angles which differ appreciably from the tetrahedral angle of 109.5° are C(1)-O(5)-C(5) and C(4)-C(5)-C(6), the former being 124°, substantially larger than the 114° found in α -D-glucose.

The conformation of six-membered rings involving a planar group has been studied by Mathieson.⁴⁷ Either a boat or a half-chair conformation is possible with a planar restraint on four of the six ring atoms. The planarity of the $\text{C}-\overset{\ominus}{\underset{\text{O}}{\text{C}}}-\text{O}-\text{C}$ group is associated with the valence bond contribution of the resonance form $\text{C}-\overset{\ominus}{\underset{\text{O}^-}{\text{C}}}=\overset{\oplus}{\text{O}}-\text{C}$. From geometrical considerations it was suggested that rings containing the carbon-carbon double bond would assume the half-chair conformation⁴⁸ while those containing the lactone group would assume a boat conformation.⁴⁹ The conformation of δ -lactones has since been studied by Cheung, Overton and Sim.⁵⁰ They confirmed the

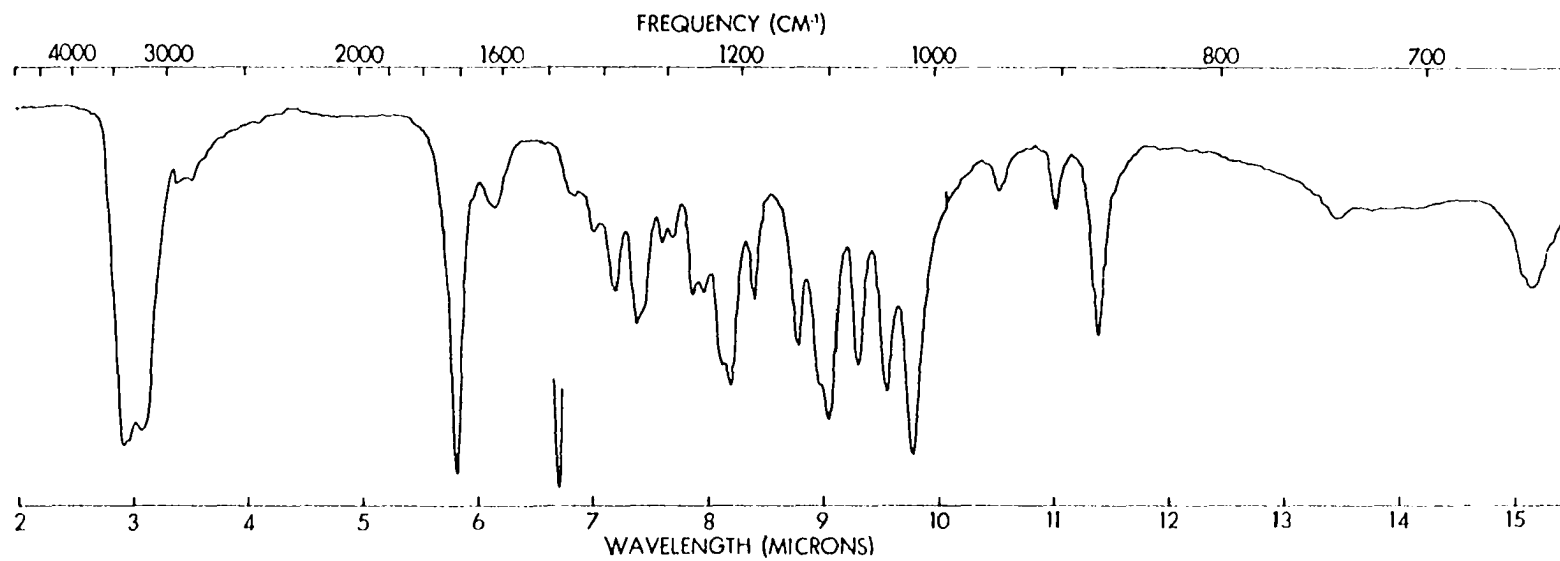


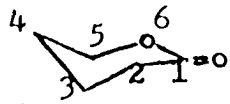

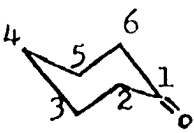
Figure 16. Infrared spectrum of D-glucono-(1,5)-lactone (KBr pellet used)

planarity of the lactone group but suggested both the boat and half-chair conformations satisfy this condition in the δ -lactones.

For glucono- δ -lactone the lactone group carbon C(5) is 0.28Å out of the best least squares carbonyl plane formed by atoms C(1), O(1), C(2), and O(5) which are planar within 0.02Å (Table 9). This non-planarity of the lactone group has also been reported by Jeffrey⁵¹ for certain γ -lactones. For ring systems where the base atoms are not coplanar, the ring is best characterized by its dihedral angles, φ . Using the ring of cyclohexane ($\varphi = 54.5^\circ$) as a reference, a molecule may be termed "flattened" or "puckered," depending upon whether φ is less than or greater than 54.5° .⁵² Comparison of the dihedral angles of various chair forms given in Table 10 indicates that the ring conformation of D-glucono-(1,5)-lactone can be best described as a distorted half-chair. The "puckering" distortions are caused by the short bonds C(1)-O(5) and O(5)-C(5) (short compared to a C-C single bond), while the large C(5)-O(5)-C(1) angle allows for some "flattening." The requirements for minimum configuration energy are met by lowering C(5) out of and C(4) nearer to the carbonyl plane resulting in a distorted half-chair conformation.

The crystal structure of D-glucono-(1,5)-lactone is shown in Figure 17. As indicated from the equation of the best least-squares plane, the normal of the plane is nearly parallel with the x-direction. The molecular packing in the crystal is largely dictated by intermolecular hydrogen bonds. There is also some ordering of the lactone dipoles in the x-direction, although the approximate separation of $a/2 = 3.9\text{\AA}$ is so large that this effect is probably minor. The infrared spectrum contains

Table 10. Dihedral angles^a (°)

	Compound	$\varphi(1,2)$	$\varphi(2,3)$	$\varphi(3,4)$	$\varphi(4,5)$	$\varphi(5,6)$	$\varphi(6,1)$
(1)		24.8(3)	47.3(3)	61.7(2)	50.9(3)	28.2(3)	15.2(4)
(2) ^b		17.2	50.2	69.0	52.7	23.5	4.2
(3) ^c		43.6(8)	54.8(7)	60.9(6)	56.3(7)	48.3(8)	40.8(8)

^aThe dihedral angle, φ , for a sixfold symmetric molecule with internal bond angles, θ , is given by

$$\cos\varphi = -\cos\theta/(1 + \cos\theta) \quad .$$

For cyclohexane ($\theta = 111.5^\circ$), $\varphi = 54.5^\circ$.

^bFrom pentachlorocyclohexene, Pasternak (1951).⁴⁸

^cFrom 4,4-diphenylcyclohexanone, Lambert, et al. (1969).⁵²

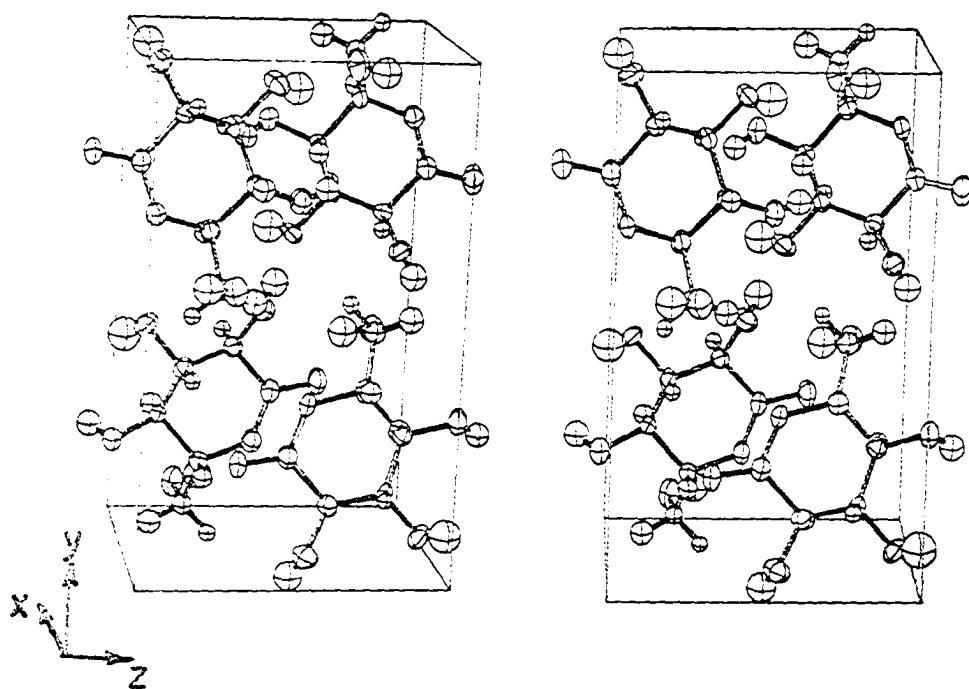


Figure 17. Stereogram of unit cell showing packing of the δ -lactone units

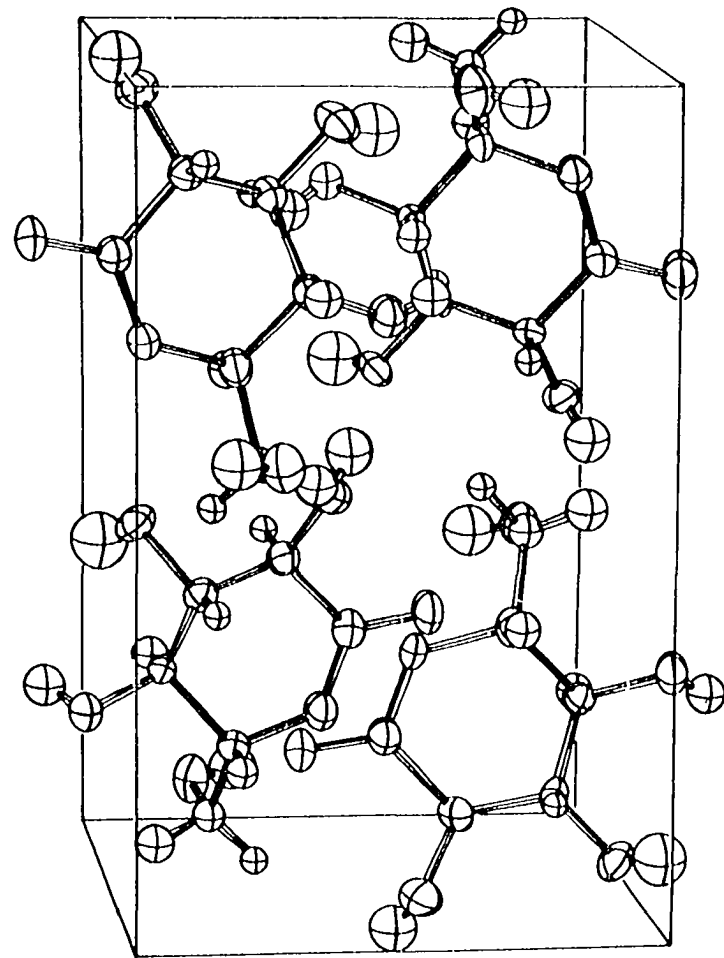
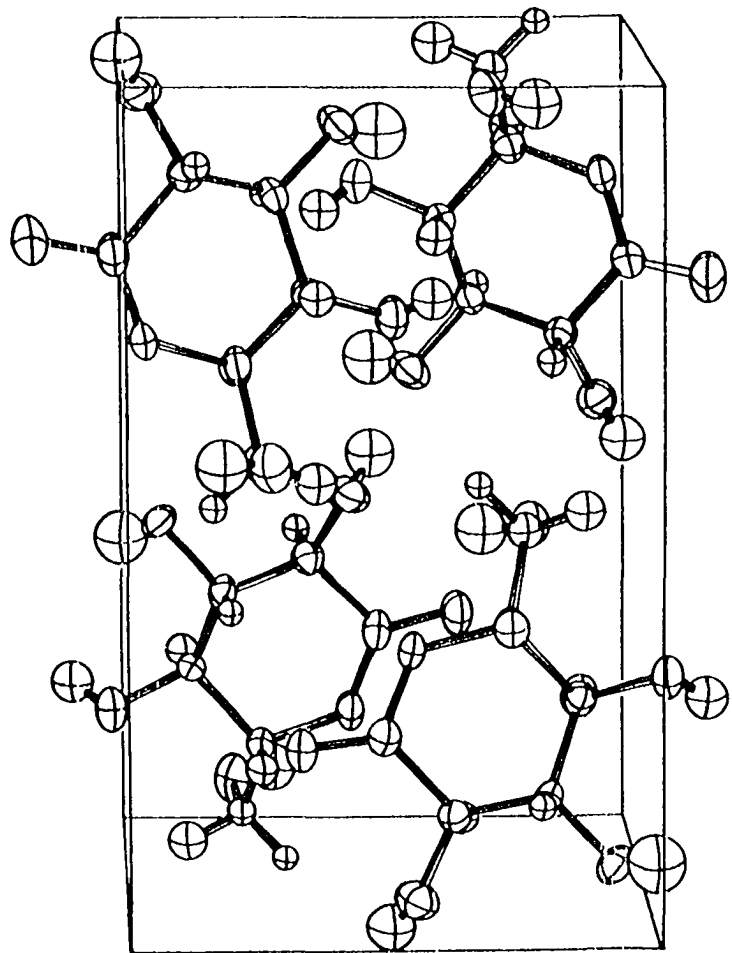


Figure 17 (continued) Cross eyes to view stereogram

a broad absorption band below 3500 cm^{-1} instead of between 3500 and 3700 cm^{-1} expected for unbound O-H groups. This is in agreement with the X-ray results which indicate a complete system of hydrogen bonds propagating three-dimensionally as shown in Figure 18. The O--O lengths range from 2.68 to 2.88\AA in good agreement with a plot of stretching frequency vs. the O--O distance given by Nakamoto, Margoshes, and Rundle.⁵³ The O-H groups bound to carbons C(2), C(3), and C(6) participate in two hydrogen bonds, acting as a donor in one and acceptor in another. The C(4) O-H group acts only as a donor in a hydrogen bond involving an O(1) atom of an identically oriented molecule at a unit cell translation in the z-direction. Each molecule is hydrogen bonded to eight surrounding neighbors. The appropriate distances and angles are given in Table 11. It should be remembered that the angles given are based on the rather short O-H distances obtained by refining the X-ray data. Note that the H---Y-M angles somewhat approximate that expected for a distorted tetrahedral angle.

Discussion

Inhibition studies of glycosidases have shown that the corresponding δ -aldonolactones are generally more efficient inhibitors than are the γ -lactones.^{54,55} Certain polyols have also been found by Kelemen and Whelan⁵⁶ to inhibit glucosidases, the most effective having a configuration similar to glucose between C(3) and C(6). Glucose also inhibits glucosidase activity, but Heyworth and Walker⁵⁷ reported that the enzyme has a relatively low affinity for glucose compared to the glucono- δ -lactone.

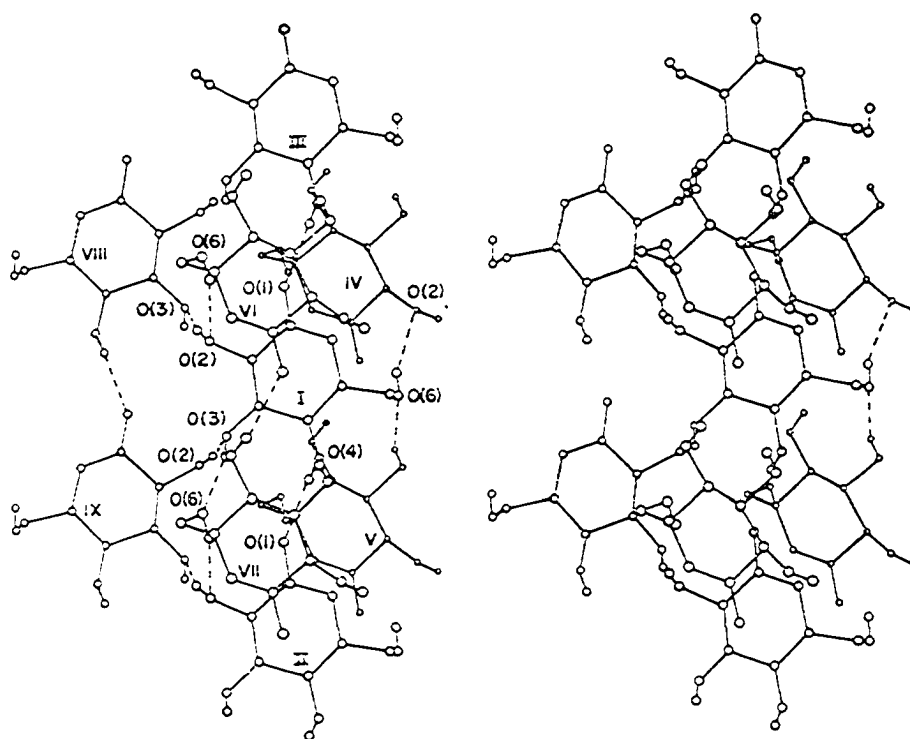


Figure 16. Stereogram of hydrogen bonding in D-glucono-(1,5)-lactone showing molecule and its eight hydrogen bond neighbors

I x, y, z

II	$x,$	$y,$	$1 + z$	VI	$-\frac{1}{2} + x,$	$\frac{1}{2} - y,$	$1 - z$
III	$x,$	$y,$	$-1 + z$	VII	$-\frac{1}{2} + x,$	$\frac{1}{2} - y,$	$2 - z$
IV	$\frac{1}{2} + x,$	$\frac{1}{2} - y,$	$1 + z$	VIII	$\frac{1}{2} - x,$	$-y,$	$-\frac{1}{2} + z$
V	$\frac{1}{2} + x,$	$\frac{1}{2} - y,$	$2 - z$	IX	$\frac{1}{2} - x,$	$-y,$	$\frac{1}{2} + z$

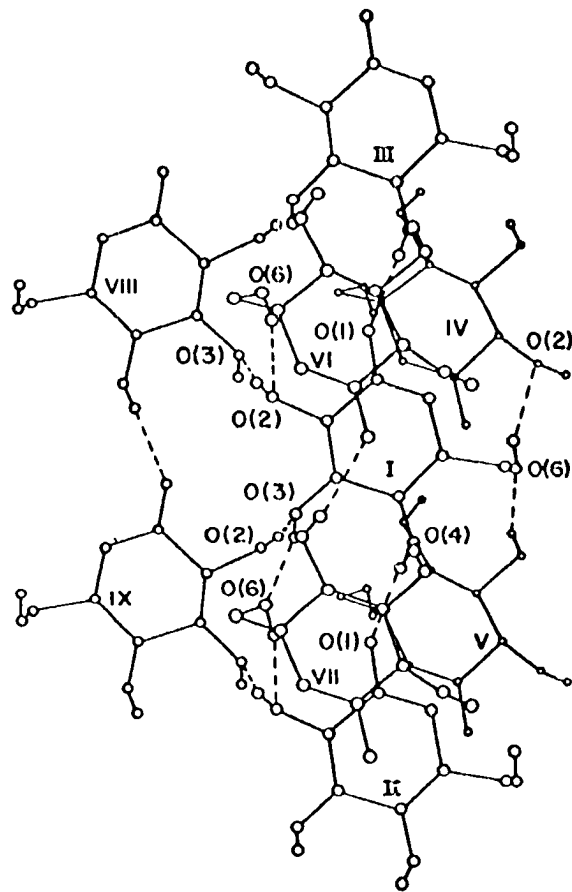
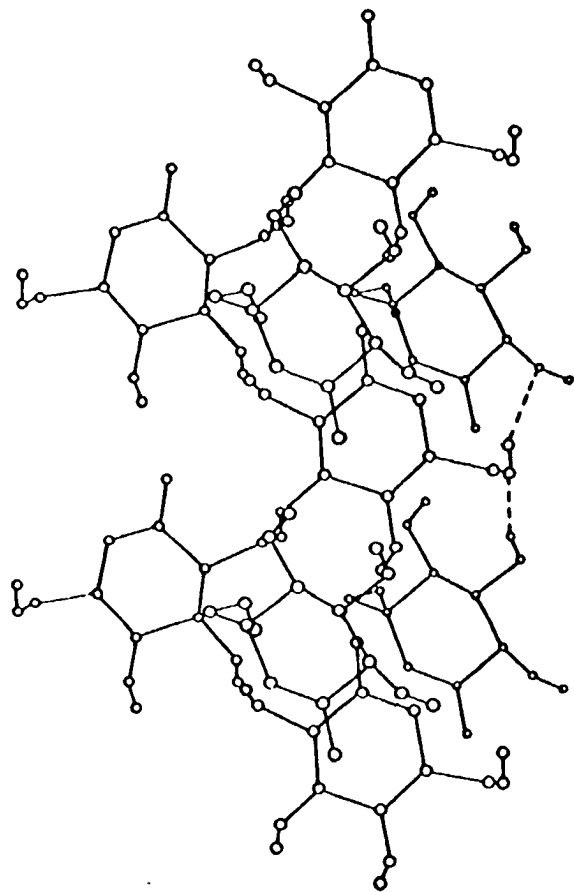


Figure 18 (continued) Cross eyes to view stereogram

Table 11. Hydrogen bonds^a in D-glucono-(1,5)-lactone

Bond X-H---Y-M	Distance (Å)			Angle (°)	
	X-H	H---Y	X---Y	X-H---Y	H---Y-M
O(2) _I -H(2') _I ---O(3) _{VIII} -C(3) _{VIII}	0.78(3)	1.98(3)	2.720(3)	160(3)	132(1)
O(3) _I -H(3') _I ---O(6) _{VII} -C(6) _{VII}	0.71(3)	2.01(4)	2.680(3)	157(4)	131(1)
O(4) _I -H(4') _I ---O(1) _{III} -C(1) _{III}	0.73(3)	2.12(3)	2.849(3)	171(3)	136(1)
O(6) _I -H(6') _I ---O(2) _{IV} -C(2) _{IV}	0.76(3)	2.15(4)	2.882(3)	162(3)	119(1)

^aRefer to Figure 18 for symmetry operation codes and stereogram of hydrogen bonding.

Leback⁵⁸ has recently reaffirmed that the specificity and high affinity of the lactone for the enzyme probably arises from the conformational similarities between the lactone and the transition state of the normal substrate. Leback also concluded that the high affinity of glycosidases for the corresponding δ -lactones is not a consequence of the lactone group itself, but of some property which it conferred to the ring. It was postulated that the transition state involved an oxy-carbonium ion in a half-chair pyranose ring. This half-chair conformation was also expected for the δ -lactone ring. The results of this investigation provide detailed structural information about this important inhibitor and establish the stable conformation of the glucose half-chair ring.

A METHOD FOR PARTIAL STRUCTURE EVALUATION

Introduction

The crystallographer has at his disposal today a number of techniques to obtain trial structures, including direct methods such as symbolic addition⁵⁹ as well as such indirect ones as Patterson superposition techniques and others discussed in the preceding chapters. (For noncentrosymmetric crystals^{60,61} a partial structure rather than a complete one is most often obtained from the symbolic addition phase determination procedure.) However, using any of these techniques with reasonably complex structures, the investigator usually finds that a number of decisions must be made regarding peaks on resultant maps as to whether or not such peaks really belong in the structure or are just spurious. The usual crystallographic discrepancy index or R factor, $R = (\sum ||F^o| - |F^c||) / \sum |F^o|$ is often of little help in this regard except to indicate when nearly all atoms have been placed in reasonably correct positions. A much more valuable function would be one which could be used to test a structural fragment of any size--a type of discriminator function which could be used to test whether each atom or group of atoms as they are added in turn appear to be correct. Such a function would enable the investigator to test structural fragments obtained from the interpretation of the Patterson function, tentative atom positions to be used in superposition procedures, the various peaks appearing in an electron density map incompletely phased with too small a fragment, or the set of peaks occurring in an E-map computed from one of several possible sign combinations.

The Discriminator Function

One of the tests that can be used to evaluate the correctness of a structure is to compare the agreement between the calculated and observed Patterson functions. The method of vector verification^{39,40} does this in checking that the vector set resulting from a tentative atom position is actually present in the observed Patterson. In fact, minimizing the quantity $(P^o - P^c)^2$ is similar to a least-squares refinement based on intensities.

For a correct arrangement of n atoms, for every peak in P_n^c , the calculated Patterson of a fragment of n atoms, there must be a corresponding peak in the observed Patterson, P^o . Theoretically, there would be no areas in the difference Patterson which would be negative. Thus a necessary condition that the atoms in the fragment are correctly placed is that

$$S_n^o = \int |P^o - P_n^c| dv$$

be a minimum. (An absolute value rather than a square function is used since a Patterson function commonly contains multiple peaks.) For a correct fragment there should be no negative regions in the difference Patterson. We can therefore ignore the absolute value in evaluating the integral and the expected minimum value can thus be readily calculated for any choice of the n fragment. If there are N atoms in the unit cell and n atoms in the selected fragment,

$$S_n^c = (\sum_i^N Z_i)^2 - (\sum_i^n Z_i)^2 = F_N^c(000)^2 - F_n^c(000)^2 .$$

That is, S_n^c would be equal to the sum over all $Z_i Z_j$ interactions between all atoms in the unit cell minus the sum over all $Z_i Z_j$ interactions between atoms in the n fragment. Since the theoretical value of S can be defined

and evaluated for a correct arrangement of atoms in the fragment, it is thus possible to define a discriminator index which allows an investigator to test whether a particular atom or fragment is incorrect. The discriminator index can be defined as

$$D = \frac{\Delta S^c - \Delta S^o}{\Delta S^c}$$

where ΔS^c is the theoretical change expected in S when atoms are in correct positions, and ΔS^o is the actual change in S that is observed. Thus if $n - n'$ atoms are added to a small fragment of n' atoms that have been placed correctly, the expected decrease in S is given by

$$\Delta S^c = S_n^c - S_{n'}^c = F_n^c(000)^2 - F_{n'}^c(000)^2 .$$

If these additional atoms are also placed in correct positions, the observed change in S,

$$\Delta S^o = S_n^o - S_{n'}^o ,$$

will be approximately equal to ΔS^c . Thus for a correct addition to the n' atom fragment, a D value of approximately zero would be expected. If, however, the $n - n'$ atoms are placed in random positions and the Patterson peaks are reasonably sharp, it would be expected that the value of S_n^o will nearly equal that of $S_{n'}^o$, that $\Delta S^o \approx 0.00$; thus $D \approx 1.00$.

The starting fragment may be chosen from the result of superpositions, from an electron density map computed from an initial set of phases determined from direct methods, or by any other available method. Note that no assumptions have been made regarding the size of the fragment considered; thus, it is theoretically possible to use the discriminator function to test each atom of the asymmetric unit as it is added even in the very early stages of solution where the R factor is most insensitive. In fact, one

would usually begin with $n' = 0$ to test the starting fragment upon which to build. The method therefore extends the idea of vector verification by considering the size and shape of a peak as well as its location and also provides an index to judge the results.

The importance of the size and shape of a peak as well as its position when using the discriminator function for partial structure evaluation is illustrated in Figure 19 using the hypothetical carbon monoxide example. As shown, integration of a single peak in electron density space (a) equals the Z_i value associated with that peak and integration over the entire unit cell gives the sum of all Z_i or the $F_N(000)$ value for the structure. Integration of a single peak in Patterson space (b) equals the $Z_i Z_j$ value of the atoms whose interatomic vector corresponds to that Patterson peak position, while integration over the entire unit cell equals the sum of all $Z_i Z_j$ interactions or the value of $F_N(000)^2$ for the structure. Now consider testing an oxygen starting fragment, using the possible coordinates determined from the peaks on the Harker section at $y = 1/2$. The calculated Pattersons for the oxygen in its correct position (c) and in the carbon's position (d) both integrate to the value of $F_N^c(000)^2$; however, the values of the integrals over the absolute value of the corresponding difference Pattersons (e,f) are quite different. For the correct oxygen position the corresponding 0-0 peaks are present in both maps so the discriminator index is 0.00. However, in the case where the oxygen is improperly placed in the carbon position, the peaks in the observed and calculated maps do not match in size and the D index is 0.44. The D index would have been substantially higher had an incorrect position for an atom been tested, although there will always be some fit because of the origin peak.

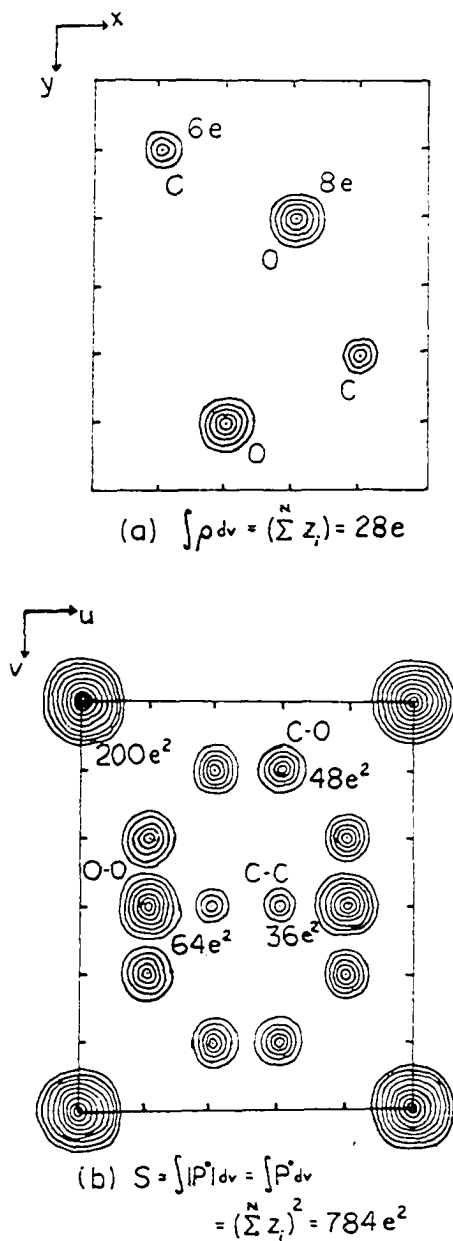


Figure 19. An illustration of the use of the discriminator function to distinguish the carbon and oxygen positions in the hypothetical CO example: a) electron density map; b) Patterson map;

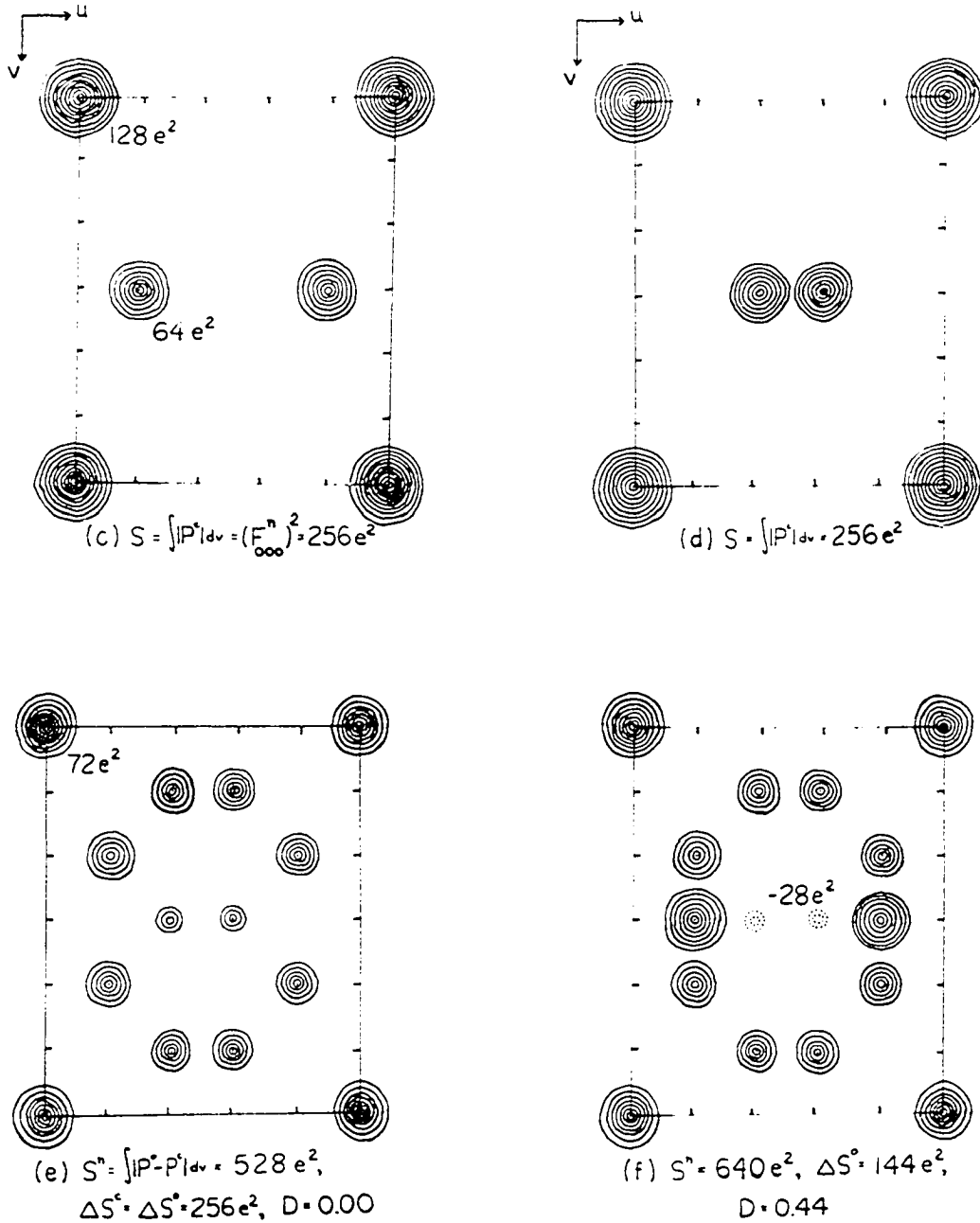


Figure 19 (continued)

c) and d) calculated Patterson maps for the oxygen fragment; and
 e) and f) the corresponding difference Pattersons with D index

Experimental

The method was tested by taking advantage of existing programs which could be easily modified to do the necessary computations. A modified version of OR FLS was used to compute the calculated structure factors. It was, of course, necessary to use a complete set of data, including the unobserved and the $F(000)$ reflections, placing all data on the absolute scale. However, it has been found in practice that for most cases, sufficiently accurate scale factor and thermal parameters can be obtained from a Wilson plot. The data set containing the F^o 's and F^c 's was passed to a second program where sharpened coefficients were computed by

$$\underline{F}_{hkl}^s \quad ^2 = (\underline{F}_{hkl}^o / k\hat{f})^2 \exp[-(2B-B') \sin^2 \theta / \lambda^2]$$

where $\hat{f} = \sum f_j / \sum Z_j$, B is the overall isotropic temperature factor, and B' is a variable used to minimize rippling due to non-termination of series effects. The use of a sharpened Patterson is often desirable, particularly in light or equal atom cases, to improve the sensitivity to make a low D index not only a necessary but also a sufficient condition for the correctness of the partial structure being tested. The measured intensity of all unobserved reflections was set to zero to avoid introducing magnified errors after sharpening. The difference coefficients were then passed to the ALFFDP (Ames Lab Fast Fourier Difference Patterson) program where the numerical approximation for S at roughly $1/4\text{\AA}$ resolution and D index for a monoclinic map of $32 \times 32 \times 32$ grid size can be computed in less than 20 sec. This procedure, although simple to use and modify to each particular case, does restrict one to a point by point method for testing tentative atom positions.

Results

To explore the applicability of the discriminator function, it was tested extensively on D-glucono-(1,5)-lactone, which crystallizes in the orthorhombic space group $P2_12_12_1$ with $Z = 4$. The structure was solved by symmetry map--Patterson map superpositions. For this case, sharpened data ($2B-B^* = 2.0\text{\AA}^2$) were used with fixed estimates for the scale factor and thermal parameters ($k = 1.70$, $B = 2.5\text{\AA}^2$). The necessary condition that S be a minimum for a correct fragment was tested by building up a fragment of the gluconolactone molecule. Since there are four equivalent positions, the size of the fragment increases by four for each new atom added. The starting point was taken as the integral over the absolute value of a sharpened Patterson, the value obtained being approximately 4% greater than the $141,376e^2$ theoretically expected ($F(000) = 376e$). In Table 12 are shown the results obtained for increasing the size of the fragment one atom/molecule at a time. The notation used in this and subsequent tables includes the n' fragment, which is the assumed correct fragment, with the $+n$ th atoms being those tested. Note that although only the unique atoms of the asymmetric unit are listed, the fragments also include the symmetry related atoms. In every case low D values were obtained, indicating good agreement with the observed Patterson. Note that the magnitude of ΔS^C increases rapidly with the size of the fragment tested.

In order for the discriminator to be useful, it is necessary that a minimum value of S be not only a necessary but also, in practice, a sufficient condition that atoms in a fragment be correctly positioned.

Table 12. Discriminator values for correct fragments

n' Fragment ^a	+ nth	ΔS^c	S_n^o	D	R
-	-	-	147042	-	-
-	01	1024	145969	-0.05	0.75
01,	05	3072	143135	0.08	0.68
01,05,	C1	3648	139963	0.13	0.64
01,05,C1,	C5	4800	135567	0.08	0.61
01 - C1,C5,	C4	5952	130151	0.09	0.58
01 - C5,C4,	C3	7104	123236	0.03	0.54
01 - C4,C3,	C2	8256	115614	0.08	0.51
01 - C3,C2,	C6	9408	107112	0.10	0.48
01 - C2,C6,	02	14336	93830	0.07	0.43
01 - C6,02,	03	16384	79058	0.10	0.37
01 - 02,03,	04	18432	63542	0.16	0.30
01 - 03,04,	06	20480	46325	0.16	0.18

^aCarbons and oxygens are numbered consecutively from the carbonyl group.

The results obtained when incorrect peak positions were tested are shown in Table 13. In general, these positions were selected from peaks remaining on a map obtained from a set of four symmetry map--Patterson map superpositions, and thus partial fitting of the observed Patterson would be expected. These values are all significantly higher than those in Table 12. Also note that the difference in D values for a given n' fragment is much more noticeable than the corresponding changes in the R-factors, particularly for the small fragment sizes. Thus it would be very difficult to distinguish between these positions using the usual R factor.

The results shown in Tables 12 and 13 were obtained using least-squares fitted positional parameters for the various atoms in the correct fragment. The sensitivities of S and the discriminator index D to exact positioning are shown in Table 14. Note that minimizing S corresponds to improving the trial position of the atom added to the fragment while again the R-factor is relatively insensitive. Since the values obtained are dependent on the size of the peaks in the sharpened Patterson, one might well expect that the degree of sensitivity could be adjusted by modifying the thermal coefficient used in computing the sharpened coefficients. Indeed this is the case, as shown in Table 15. As expected, reducing the thermal parameter results in broader peaks that are more easily fitted, and increasing the thermal parameter results in sharper peaks with increased sensitivity. Note, however, that with correct positioning the D values are similarly low for either degree of sharpening.

In all the results presented thus far, a fixed scale factor was used which was close to the final least-squares scale factor. Since in practice

Table 13. Discriminator values for incorrect fragment additions

n' Fragment	+nth	D	R
01,	O* ^a	0.82	0.72
01,05,	O*	0.68	0.64
01,05,C1,	C*	0.52	0.64
"	C*	0.47	0.62
"	C*	0.40	0.62
"	O*	0.71	0.63
"	O*	0.59	0.61
01 - C1,05,	C*	0.42	0.59
01 - C5,C4,	C*	0.50	0.56
01 - C4,C2,	C*	0.49	0.53
01 - O3,O4	O*	1.24	0.36

^aAsterisk indicates atom position selected from different spurious peaks on resultant superposition map.

Table 14. Sensitivity to correct positioning

(n' Fragment--01,05,C1,; + nth--03)		
Displacement(Å)	D	R
0.0	0.03	0.59
0.118	0.10	0.59
0.185	0.19	0.60
0.370	0.37	0.61
0.113	0.08	0.59
0.226	0.18	0.59
0.339	0.29	0.60

Table 15. Dependence of sensitivity on thermal coefficient used in sharpening

(n' Fragment--01 - 05,C4,; + nth--C3)			
Displacement(Å)	D ^a	D ^b	R
0.0	0.02	0.00	0.54
0.123	0.03	0.07	0.54
0.246	0.06	0.28	0.55
0.370	0.13	0.52	0.56

$${}^a_{2B} - B' = 1.0\text{Å}^2.$$

$${}^b_{2B} - B' = 3.0\text{Å}^2.$$

scale factors can not usually be estimated to much better than 10% accuracy, in Table 16 are additional values of S and D computed with slightly erroneous scale factors. Comparing these results and those in Table 12, it is noticed that although the value of S varies appreciably, the D factors are very similar, low D values being obtained for correct additions to the starting fragment and high D values being obtained for incorrect additions in both cases.

The first results obtained during an actual structural determination were on 1,1-dimethyl-2,5-diphenyl-1-silacyclopentadiene photo-dimer (silole dimer)⁶² which crystallizes in space group $P\bar{1}$ with $Z = 2$. This molecule contains 36 carbons and 2 silicons plus hydrogens, $F(000) = 560e$. The results shown in Table 17 were obtained using sharpened data ($2B - B' = 1.0\text{\AA}^2$) and fixed estimates for the scale factor and thermal parameters ($k = 4.35$, $B_{Si} = 3.0\text{\AA}^2$, $B_C = 4.0\text{\AA}^2$). The linear fit of the Wilson plot obtained in this case was extremely poor. The variation of S with scale factor was therefore examined to attempt to obtain a more reasonable estimate of the scale factor, the rationale being that the integral over the absolute value of the observed Patterson will increase rapidly when k is too small (structure factor amplitudes too large), but will decrease only very slightly as k becomes too large. The results are plotted in Figure 20. The value of 4.35 was chosen from the plot and the value of the starting integral obtained using this scale factor was only a percent higher than the $313,600e^2$ theoretically expected. The silicon positions were obtained from a sharpened Patterson and then tested with the discriminator giving a low D index of -0.02. A silicon phased electron density map was next computed which contained many extra peaks. These

Table 16. Sensitivity to improper scaling of F^0 's

n' Fragment	+nth	S^a	D	R	S^b	D	R
-	-	151624	-	-	144412	-	-
-	01	150632	0.03	0.74	143487	0.10	0.71
01,	05	147667	0.03	0.66	140680	0.09	0.64
01,05,	C1	144516	0.14	0.64	137533	0.14	0.62
01,05,C1,	C5	140282	0.12	0.62	133085	0.07	0.59
01 - C1,C5,	C4	134830	0.08	0.58	127479	0.06	0.56
01 - C5,C4,	C3	128093	0.05	0.55	120500	0.02	0.53
01,05,C1,	C*	142219	0.52	0.61	134925	0.46	0.60
01 - C5,C4,	C*	132328	0.65	0.56	124567	0.59	0.55

$$^a_k = 1.60.$$

$$^b_k = 1.80.$$

Table 17. Discriminator results on silole dimer^a

n' Fragment	+nth	ΔS^c	S_n^o	D	R
--	--	--	316743	--	--
--	Si1, Si2	3136	313549	-0.02	0.62
Si1, Si2,	C1	1488	312135	0.05	0.61
"	C5	"	312132	0.05	0.62
"	C35	"	312121	0.04	0.62
"	C*	"	313369	0.88	0.62
"	C*	"	312705	0.43	0.62
"	C1, C5, C35	5328	315518	-0.02	0.59
Si1 - C35,	C7	2352	313176	0.00	0.58
"	C8	"	313162	-0.00	0.58
"	C9	"	313247	0.03	0.59
"	C26*	"	313664	0.21	0.59
"	C*	"	313945	0.33	0.59
"	C*, C7, C8, C9	11136	306311	0.17	0.57
"	C13, C14, C15, C16	"	304709	0.03	0.57

^aCarbon coordinates were taken from the silicon phased electron density map.

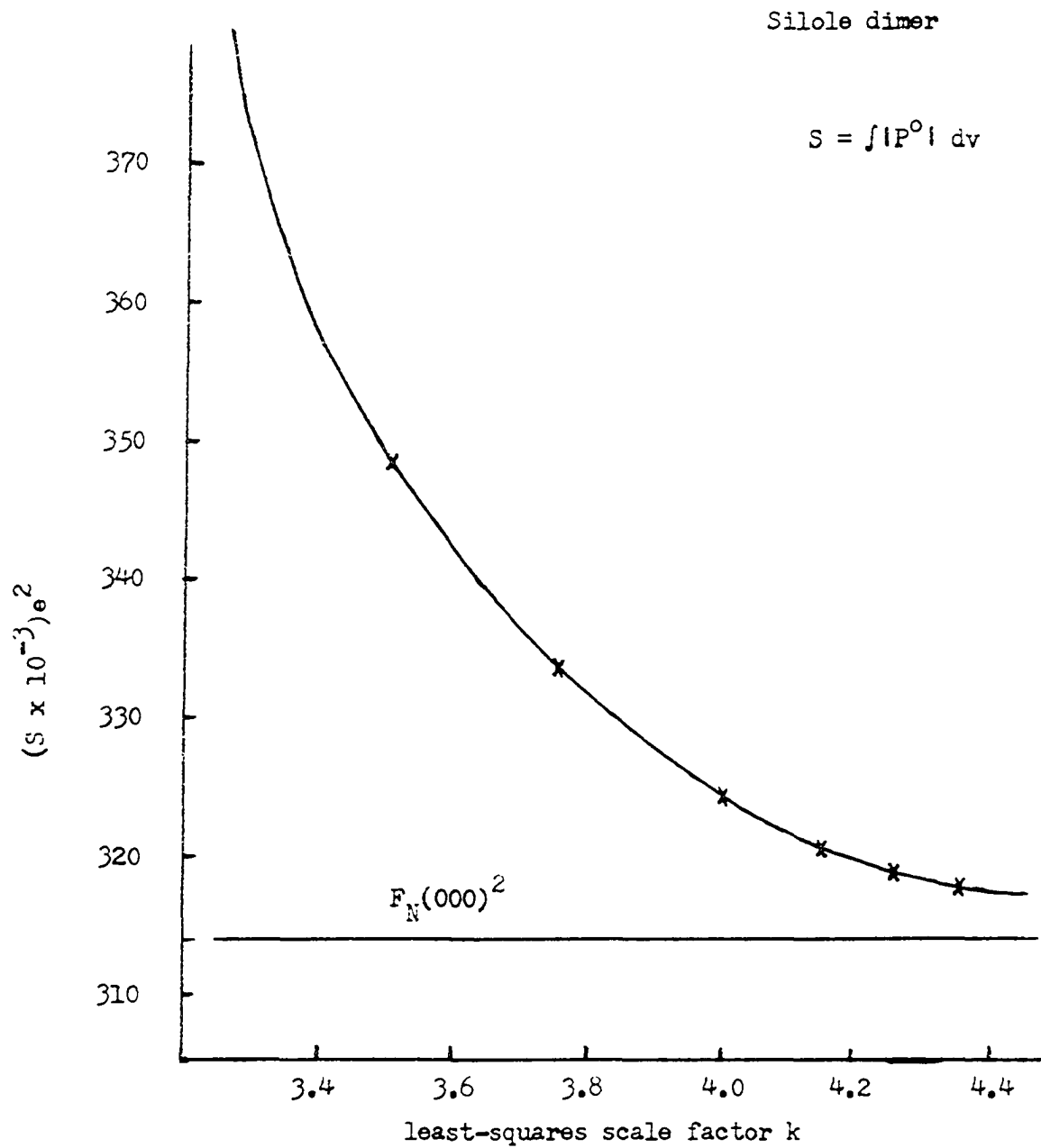


Figure 20. Variation of the integral over the absolute value of the observed Patterson as a function of scale factor

positions were tested in turn, with low D values being obtained for what later turned out to be correct atom positions and higher D values obtained for incorrect positions. Note again that the R-factor is relatively insensitive for fragments of this size making it difficult to distinguish these positions.

The discriminator was next used in conjunction with the structural investigation of $\text{Cs}_3\text{Sb}_2\text{Cl}_9$ ⁶³ which crystallizes in space group *Pnma* with $Z = 4$. The Patterson of this structure was somewhat unusual in that all peaks occurred at coordinates which were multiples of $1/4$ in \underline{v} , and multiples of $1/12$ in \underline{u} and \underline{w} . The integral over the absolute value of the observed Patterson was computed and found to be nearly double that theoretically expected for four formula units per cell. As this seemed unreasonable in light of the previous results, a scale factor was determined using the method described for the silole dimer. Although the scale factor obtained in this manner gave a reasonable value for the integral, it was obvious from the percentage reduction in the origin peak of the first difference Patterson that this value of k was too large. It was now apparent that the problem of the too large integral values was due to large rippling in the background caused by the unusual symmetry and heavy atom nature of this problem. It was therefore decided to examine the variation of the integral over the origin peak as a function of scale factor. The shortest bond distance expected in $\text{Cs}_3\text{Sb}_2\text{Cl}_9$ was greater than 2.5\AA , so the integration of the origin peak was carried out to a radius of approximately 1\AA . The results obtained are plotted in Figure 21. The value of 0.242 chosen from the plot compares favorably with $k = 0.248$ obtained later by least-squares refinement of the correct model structure. A single differ-

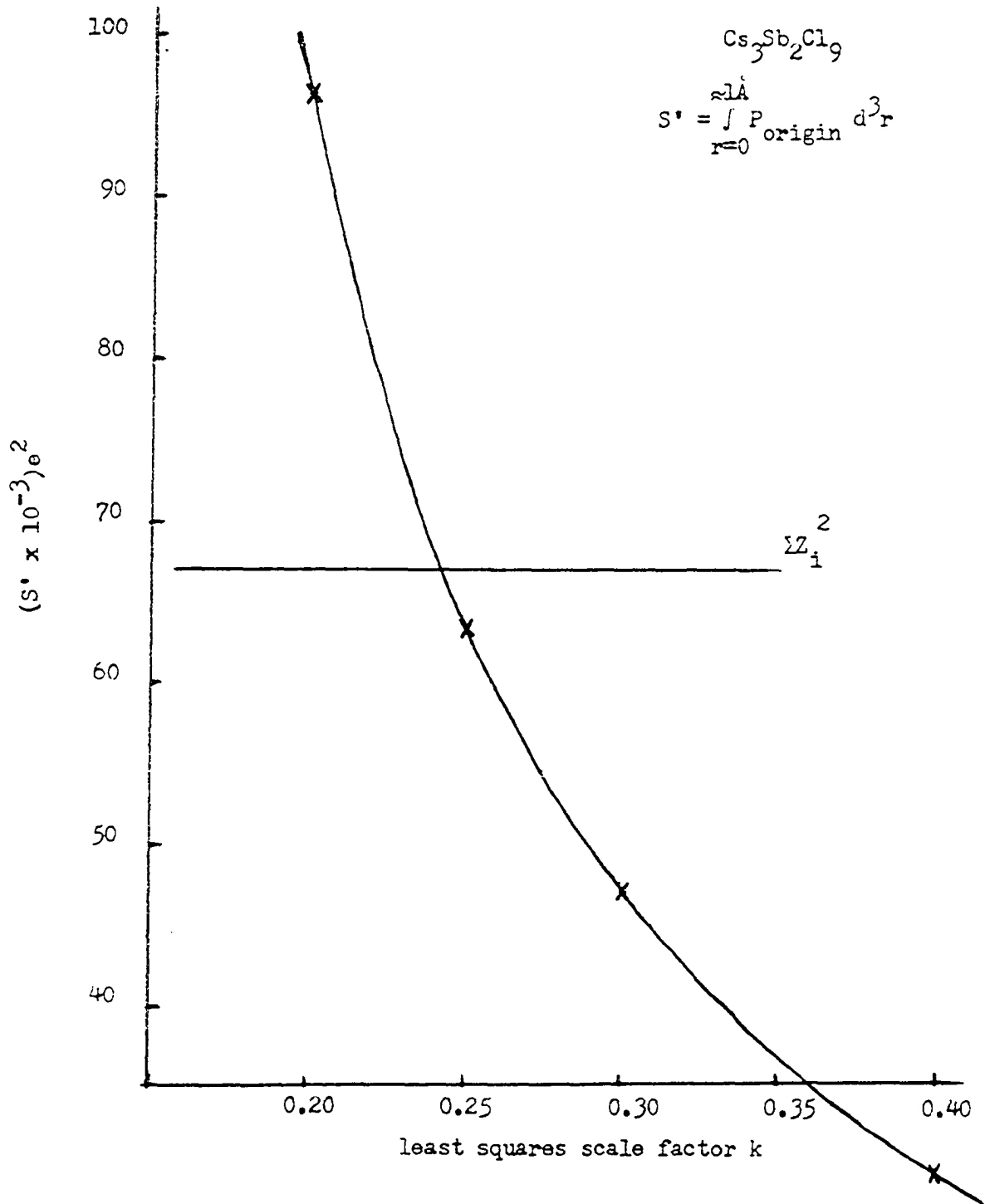


Figure 21. Variation of the integral over the origin peak as a function of scale factor

ence Patterson was computed using this scale factor. Examination of the resulting map eliminated from consideration two of the three sets of special positions in which the heavy atoms were expected to lie. The structure was then solved by direct methods and confirmed that all heavy atoms lie on the mirror planes as required by this third remaining set of special positions.

The problems encountered in the $\text{Cs}_3\text{Sb}_2\text{Cl}_9$ structure led to further testing of the method on the inorganic compound Ag_2CrO_4 ,⁶⁴ which also crystallizes in space group Pnma , $Z = 4$, and $F(000) = 600e$. This structure contains both heavy and light atoms with the heavy atoms occupying special positions. This structure can be and was solved in a straight forward manner by analyzing the Patterson. However, it is a good test case since it is similar to the $\text{Cs}_3\text{Sb}_2\text{Cl}_9$ problem but represents quite a different type of problem from the all light atom, rather low symmetry problems of the lactone and silole dimer. The results obtained are given in Table 18. The first set of data was obtained using fixed estimates for the scale factor and thermal parameters, but now using unsharpened data. The integral was still high, but by only about 5 percent. Note that for such structures where there are relatively few independent heavy atoms the R-factor is fairly sensitive to correct additions to the fragment. However, the point to be made is that the discriminator is also sensitive and should remain sensitive so as to work equally well for those problems involving a large number of heavy atoms where the R-factor would again be insensitive. The last three values given in the table were obtained using sharpened data. In this case, the value of the integral had increased markedly due to sharpening, but again the D values are still low for correct additions to the fragment.

Table 18. Discriminator results on silver chromate

n ^o Fragment	+nth	ΔS^c	S_n^o	D	R
--	--	---	374705	--	--
--	Agl	35344	337825	-0.04	0.65
--	Ag*	"	350877	0.33	0.75
Agl,	Ag2	106032	227593	-0.04	0.41
Agl,Ag2,	Cr	81408	149202	0.04	0.22
"	Cr*	"	213507	0.83	0.42
--	--	---	436478	--	--
--	Agl,Ag2	141376	290541	-0.03	0.41
Agl,Ag2,	Cr	81408	210240	0.01	0.22
Agl,Ag2,Cr,	O1	31232	118712	0.02	0.21
"	O2	"	121414	0.11	0.21
"	O*	"	141913	0.77	0.22
"	O3	64512	94705	0.15	0.20
"	O1,O2,O3	137216	48309	0.26	0.16
"	O*,O*,O*	"	80379	0.50	0.22

The structure determination of the quinoline antimony bromide complex $(\text{RSbBr}_6 \cdot \text{RBr}_3, \text{P}2_1/\text{n}, Z = 2)^{65}$ represents the last type of application for which results have been obtained thus far. The positions of the heavy atom SbBr_6 and Br_3 groups were readily determined from the Patterson map. However, the electron density map produced with the heavy atom phasing contained many spurious peaks. These positions were then tested with the discriminator, with D values less than 0.18 being obtained for what later were determined to be correct atom positions and D values greater than 0.41 for what later were determined to be incorrect atom positions. The results were obtained with unsharpened data using fixed thermal parameters and the scale factor obtained from the heavy atom refinement. Again, the improved sensitivity of the discriminator index compared to the usual R-factor to distinguish correct from incorrect additions to the fragment was apparent.

Discussion

The method just described for partial structure evaluation is theoretically sound; however, it is the severity of the problems encountered in practice that determine its usefulness, and these will now be discussed along with some suggestions for surmounting, or at least minimizing, their effects. The first problem one encounters is that of obtaining a complete set of properly scaled structure factor data. A complete set of data implies all independent intensity data measured out to the $\sin\theta/\lambda$ limit feasible for the particular crystal and instrument plus the $F(000)$ reflection. Calculation of the latter requires only a knowledge of the

stoichiometry and number of formula units per cell, but it is important that it, or at least a close estimate of it, be included in the data set. The problem of proper scaling is usually more difficult; however, it would seem that a reasonable estimate, i.e., within 10%, is all that is necessary. With a good set of intensity data, satisfactory estimates for nearly equal atom problems without too much unusual molecular or crystallographic symmetry can be obtained from a Wilson plot. (The difficulty in the silole dimer problem was due to some inaccurate diffractometer data.) If the Wilson plot deviates badly from a linear fit, then the method used for the $\text{Cs}_3\text{Sb}_2\text{Cl}_9$ problem can probably provide a workable estimate. The accuracy of the thermal parameters assigned in computing the calculated structure factors also does not seem to be too much of a problem, a Wilson plot value or a common sense average based on the type of structure and degree of fall off of intensity data with $\sin\theta/\lambda$ being sufficient.

The decision whether or not to use sharpened data, and then how much thermal sharpening should be used, varies with each problem. Sharpened coefficients are used to improve the resolution of the peaks occurring in the maps so that a low D index is both a necessary and sufficient condition for correct additions to the fragment. In general, if the scale factor is known to within 10%, one should probably sharpen as much as possible but still avoid the problem of rippling effects. Problems with rippling have thus far been found only with heavy atom - lighter atom type problems. In these cases, the use of alternate sharpening techniques, e.g., derivative sharpening, or the use of origin removal may help. Also, for most of these cases one is primarily concerned in using the method only to obtain the heavy atom fragment which can then be used to phase an electron density

map calculation. For these heavy atom - heavy atom interactions, sharpening is usually unnecessary anyway. However, sharpening affects resolution and resolution determines how accurately the trial atom coordinates can be determined from the maps. Although more accurate coordinates are obtainable from sharpened maps, the discriminator index is also now more sensitive to correct positioning. This would suggest computing a D map once a small initial fragment has been found to locate all other possible atom positions and thus avoid the problem of accurately determining trial coordinates. The method of factorization and the storage of reuseable terms, e.g., the core part of the calculated structure factor, along with possible shortcuts in generating the calculated map and in computing the integral approximation, could greatly improve the efficiency of the calculation for such an array of terms over the point by point method currently used. Such a calculation would still involve large amounts of computer time; however, the calculations are simple and could be easily performed in a background mode by a slave instrumental computer during off hours, overnights and on weekends, when the usage is down.

There are alternate applications which seem feasible but have not yet been tried. The equations could be modified to permit calculation of a D index for use in orienting a known rigid group. The integration of the difference Patterson about the origin should prove more reliable than other methods based on checking for the presence of the various vector sets. The discriminator can not only be programmed to evaluate peaks occurring in resultant maps including E maps obtained by direct methods, but also to then determine the best consistent set of peaks from those having low individual D values.

The primary difficulty of the method is in maintaining both the necessary and sufficient conditions for the larger problems where the unit cell size and number of atoms per cell increases. The density of peaks in Patterson space increases with N^2 but the volume only increases with N . For large problems the peak density can become so high that, due to overlap, the background level of the Patterson might correspond to several single peak heights. In such a case it would not be difficult to fit any kind of fragment to the observed Patterson, a low D value being obtained in all instances. If the density of peaks is not too high, increased sharpening may be sufficient. For many of the larger problems, there is usually a large part of the entire molecule which has been previously determined. The use of these large fragments should also extend the size limitation for the method. An alternate approach to the problem of high peak densities is to work at decreasing the peak density before the integrals are evaluated and the discriminator index calculated. This reduction in the number of peaks occurring in the map is readily accomplished by the Patterson superposition techniques. For example, consider the case of only a single superposition using the vector formed by the tentative atom position and one of its symmetry related counterparts. The value of the integral over the resultant map, S' for a correct choice of the n th atom would be

$$S' = \int P_{\text{sup}}^0 dv = 2Z_n \int \sum_{i=1}^N [Z_i - Z_n] + \text{spurious peaks} .$$

If a fragment of $n-1$ atom are assumed correct, then the calculated map for the addition of the n th atom would be

$$S^c = \int P_{\text{sup}}^c dv = 2Z_n \int \sum_{i=1}^n [Z_i - Z_n]$$

The value of the integral over the difference superposition map, S , would be

$$S = \int |P_{\text{sup}}^{\circ} - P_{\text{sup}}^{\text{c}}| dv = 2Z_n \left(\sum_{i=n+1}^N Z_i \right) + \text{spurious peaks} .$$

Now defining

$$\Delta S^{\circ} = S' - S ,$$

we can define the discriminator index

$$D = \frac{S^{\text{c}} - \Delta S^{\circ}}{S^{\text{c}}}$$

which has the same meaning as previously. This is just one example of how the density of peaks in the maps can be reduced to extend the size of problems that can be considered. Other variations are equally valid; however, the integral approximations may become less accurate as additional superpositions are used. The key principle of the discriminator is to use all the information available about the size and shape of a peak as well as its location coupled with the symmetry information of the space group. This principle can be applied to any meaningful map to provide a quantitative method for partial structure evaluation.

RESEARCH PROPOSALS

The following research proposals concern suggestions for further work in those research areas related to the investigations reported in this thesis. No attempt is made to detail the experimental attack nor has an exhaustive examination of the literature been made regarding these proposals.

- (1) The preparation of a simple $\text{RSb}^{\text{III}}\text{Br}_6$ complex would be of interest to determine if this complex is also intensely colored. This would require a trivalent cation, preferably organic in nature and about the same size as the expected SbBr_6^{3-} species, e. g. $\left[(\text{CH}_3)_3\text{N}(\text{C}_2\text{H}_4)_2\text{N}(\text{CH}_3)_2 \right]^{3+}$. An accurate structural investigation of this complex would also be of interest to determine the nature and symmetry of the antimony bromide species and to check for any unusual bromine-bromine van der Waals contacts. In addition, a thorough study of the reflectance spectra of the various types of solid antimony bromide salts would be of interest to gain a better understanding of the nature of these compounds and to try and correlate these spectra with the variety of stoichiometries and antimony bromide species that have been obtained. It would also be worthwhile to look for possible changes in the reflectance spectra or structures of these complexes at different temperatures. Finally, it is felt that a semiempirical treatment of the bonding of the antimony halides should be carried out as soon as computationally feasible to better understand the nature and variety of these complexes.

- (2) The importance of the heavier halogens as acceptors in hydrogen bonds has not been extensively investigated. Most of the literature available on these less common types of hydrogen bonds concerns infrared spectra of amine hydrohalides. Due to the continued theoretical interest in the hydrogen bond and because of the important effects hydrogen bonds have in determining the solid state structure of many compounds, it is felt that an accurate single crystal X-ray or neutron investigation, perhaps at low temperatures, of a system similar to that of $C_7H_9NHFeBr_4$ would be of interest to obtain accurate information on bond distances and angles for these systems.
- (3) The results obtained from the structural investigation of D-glucono-(1,5)-lactone have led to much discussion. In particular, the C(1) - O(5) distance and non-planarity of the lactone group are regarded as atypical by some investigators. Accurate structural investigations of similar lactone structures would be of interest to compare the corresponding dimensions and conformational details.
- (4) It is felt that further work with the discriminator applying some of the ideas suggested in the body of this thesis could develop a method of peak evaluation which would be a valuable complementary tool for most common methods of solutions currently employed.

LITERATURE CITED

1. Patterson, A. L., Z. Krist., A 90, 517 (1935).
2. Lawton, S. L. and R. A. Jacobson, Inorg. Chem., 5, 743 (1966).
3. Hubbard, C. R. and R. A. Jacobson, Iowa Academy of Science, 75, 85 (1968).
4. Lawton, S. L. and R. A. Jacobson, Inorg. Chem., 7, 2124 (1968).
5. Porter, S. K. and R. A. Jacobson, J. Chem. Soc., Sect. A, 1356 (1970).
6. Hackert, M. L., S. L. Lawton and R. A. Jacobson, Iowa Academy of Science, 75, 97 (1968).
7. Lawton, S. L., R. A. Jacobson and R. S. Fyre, Inorg. Chem., 9, 0000 (1970).
8. Porter, S. K. and R. A. Jacobson, J. Chem. Soc., Sect. A., 1359 (1970).
9. Clark, J. R., R. A. Jacobson and R. G. Baughman, Inorg. Chim. Acta, 4, 0000 (1970).
10. Rosenheim, A. and W. Stellman, Ber. Chem. Dtsh. Ges., 34, 3377 (1901).
11. Whealy, R. D. and R. L. Yeakley, J. Inorg. Nucl. Chem., 25, 365 (1963).
12. Petzold, W., Z. Anorg. Allgem. Chem., 215, 92 (1933).
13. Williams, D. E., "LCR-2, A Fortran Lattice Constant Refinement Program," U.S. Atomic Energy Commission Report IS-1052 (Iowa State University and Institute for Atomic Research, Ames, Iowa). 1964.
14. Ozbirn, W. and R. A. Jacobson, Inorg. Chim. Acta, 4, 0000 (1970).
15. Busing, W. R. and H. A. Levy, Acta Cryst., 10, 180 (1967).
16. Wehe, D. J., W. R. Busing and H. A. Levy, "Fortran Program for Single Crystal Orienter Absorption Corrections," U.S. Atomic Energy Commission Report ORNL-TM-299 (Oak Ridge National Laboratory, Oak Ridge, Tennessee). 1962.
17. Williams, D. E. and R. E. Rundle, J. Am. Chem. Soc., 86, 1660 (1964).

18. Stout, G. H. and L. H. Jensen, "X-ray Structure Determination," The Macmillan Co., London, England, c1968.
19. Busing, W. R., K. O. Martin and H. A. Levy, "OR FLS, A Fortran Crystallographic Least-Squares Program," U.S. Atomic Energy Commission Report ORNL-TM-305 (Oak Ridge National Laboratory, Oak Ridge, Tennessee). 1962.
20. Rodgers, J. and R. A. Jacobson, "ALF, A General Fourier Program in PL I for Triclinic, Monoclinic, and Orthorhombic Space Groups," U.S. Atomic Energy Commission Report IS-2155 (Iowa State University and Institute for Atomic Research, Ames, Iowa). 1969.
21. Doyle, P. A. and P. S. Turner, Acta Cryst., A24, 390 (1968).
22. Templeton, D. H. in "International Tables for X-ray Crystallography," Vol. III, The Kynock Press, Birmingham, England, 1962, pp. 215, 216, Table 3.3.2C.
23. Johnson, C. K., "OR TEP: A Fortran Thermal-Ellipsoid Plot Program for Crystal Structure Illustrations," U.S. Atomic Energy Commission Report ORNL-3794 (Oak Ridge National Laboratory, Oak Ridge, Tennessee). 1965.
24. Busing, W. R., K. O. Martin and H. A. Levy, "OR FFE, A Fortran Crystallographic Function and Error Program," U.S. Atomic Energy Commission Report ORNL-TM-306 (Oak Ridge National Laboratory, Oak Ridge, Tennessee). 1964.
25. Pauling, L., "The Nature of the Chemical Bond," Cornell University Press, Ithaca, N.Y., 1960, p. 260.
26. Stucky, G. D., J. B. Folkers and T. J. Kistenmacher, Acta Cryst., 23, 1064 (1967).
27. Clausen, C. A., III and M. L. Good, Inorg. Chem., 8, 220 (1969).
28. Wrinch, D. M., Phil. Mag., 27, 98 (1939).
29. Buerger, M. J., Acta Cryst., 3, 87 (1950).
30. Beevers, C. A. and J. H. Robertson, Acta Cryst., 3, 164 (1950).
31. Hubbard, C. R. and R. A. Jacobson, "A Fortran IV Crystallographic System of Programs for Generalized Superpositions," U.S. Atomic Energy Commission Report IS-2210 (Iowa State University and Institute for Atomic Research, Ames, Iowa). 1970.
32. Jacobson, R. A., J. A. Wunderlich and W. N. Lipscomb, Acta Cryst., 14, 598 (1961).

33. Bak, B., L. Hansen-Nygaard and J. Rastrup-Anderson, J. Mol. Spectry., 2, 361 (1958).
34. Stewart, R. F., E. R. Davidson and W. T. Simpson, J. Chem. Phys., 42, 3175 (1965).
35. Scheringer, C., Acta Cryst., 16, 546 (1963).
36. Pimentel, G. C. and A. L. McCellan, "The Hydrogen Bond," Freeman, San Francisco, 1960, pp. 255-295.
37. Chenon, B. and C. Sandorfy, Can. J. Chem., 36, 1181 (1958).
38. Wilson, A. J. C., Nature, 150, 151 (1942).
39. Mighell, A. D. and R. A. Jacobson, Acta Cryst., 16, 443 (1963).
40. Gorres, B. T. and R. A. Jacobson, Acta Cryst., 17, 1599 (1964).
41. Simpson, P. G., R. D. Dobrott and W. N. Lipscomb, Acta Cryst., 18, 169 (1965).
42. Hamilton, W. C., Acta Cryst., 18, 866 (1965).
43. Jacobson, R. A. in "Crystallographic Computing," Munksgaard, Copenhagen, Denmark, 1970.
44. Harker, D., J. Chem. Phys., 4, 381 (1936).
45. Jensen, L. and M. Sundaralingam, Science, 145, 1185 (1964).
46. Brown, G. M. and H. A. Levy, Science, 147, 1038 (1965).
47. Mathieson, A. McL., Tetrahedron Letters, 2, 81 (1963).
48. Pasternak, R. A., Acta Cryst., 4, 316 (1951).
49. McConnell, J. F., A. McL. Mathieson and B. P. Schoenborn, Tetrahedron Letters, 10, 445 (1962).
50. Cheung, K. K., K. H. Overton and G. A. Sim, Chem. Comm., 634 (1965).
51. Jeffrey, G. A. and S. H. Kim, Chem. Comm., 211 (1966).
52. Lambert, J. B., R. E. Carhart and P. W. R. Corfield, J. Am. Chem. Soc., 91, 3567 (1969).
53. Nakamoto, K., M. Margoshes and R. E. Rundle, J. Am. Chem. Soc., 77, 6480 (1955).
54. Li, Y. -T., J. Biol. Chem., 242, 5474 (1967).

55. Conchie, J., A. L. Gelman and G. A. Levvy, Biochem. J., 103, 609 (1967).
56. Kelemen, M. V. and W. J. Whelan, Arch. Biochem. Biophys., 117, 423 (1966).
57. Heyworth, R. and P. G. Walker, Biochem. J., 83, 331 (1962).
58. Leaback, D. H., Biochem. Biophys. Res. Commun., 32, 1025 (1968).
59. Karle, I. L., K. Britts and P. Gum, Acta Cryst., 17, 496 (1964).
60. Karle, J. and I. L. Karle, Acta Cryst., 21, 849 (1966).
61. Karle, J. in "Crystallographic Computing," Munksgaard, Copenhagen, Denmark, 1970.
62. Thaxton, C. B., R. A. Jacobson and J. C. Clardy, J. Chem. Soc., Sect. A, 0000 (1971).
63. Pflaum, W. R. and R. A. Jacobson, Inorg. Chem., 10, 0000 (1971).
64. Hackert, M. L. and R. A. Jacobson, Inorg. Chem., 10, 0000 (1971).
65. McAfee, E. R. and R. A. Jacobson, Inorg. Chem., 10, 0000 (1971).

ACKNOWLEDGMENTS

For helping to make this brief stay in Ames at Iowa State University a most pleasant one, the author wishes to express his sincere appreciation to:

Prof. Robert A. Jacobson for his guidance, continued interest in, and helpful discussions concerning this work;

the State of Iowa and the United States government for financial assistance in the form of teaching and research assistantships and NSF and NDEA fellowships;

Prof. Dexter French for his suggestion of and helpful discussions concerning the D-glucono-(1,5)-lactone problem;

the faculty and graduate students for their assistance and discussions, and a special acknowledgment to the members, students and staff of X-ray Group 1;

Tim Keiderling, a summer research trainee, for his assistance with the structural determination of $(C_2H_5)_4NSbBr_6$;

Fred Hollenbeck for his advice and day to day technical assistance; and to my wife, Elaine, for her continued support during graduate school and for her help in the preparation of this manuscript.